Title

Geothermal play fairway analysis, part 1: Example from the Snake River Plain, Idaho

Authors

Shervais, John W

DeAngelo, Jacob

Glen, Jonathan M

et al.

Publication Date

2024-02-01

DOI

10.1016/j.geothermics.2023.102865

Geothermics 117 (2024) 102865

Contents lists available at ScienceDirect

Geothermics

journal homepage: www.elsevier.com/locate/geothermics

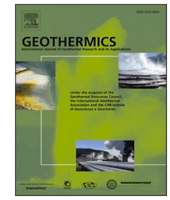

Geothermal play fairway analysis, part 1: Example from the Snake River Plain, Idaho

John W. Shervais [a,*], Jacob DeAngelo [b], Jonathan M. Glen [b], Dennis L. Nielson [c], Sabodh Garg [d], Patrick Dobson [e], Erika Gasperikova [e], Eric Sonnenthal [e], Lee M. Liberty [f], Dennis L. Newell [a], Drew Siler [b,e,1], James P. Evans [a]

[a] *Utah State University, Logan, UT 94322, USA*
[b] *U.S. Geological Survey, 350 N. Akron Road, Moffett Field, CA 94035, USA*
[c] *DOSECC Exploration Services LLC., 2075 Pioneer Rd., Suite B, Salt Lake City, UT 84104, USA*
[d] *Geologica Geothermal Group, Inc, 9920 Pacific Heights Blvd, Suite 150, San Diego, CA 92121, USA*
[e] *Lawrence Berkeley National Laboratory, 1 Cyclotron Road, Berkeley, CA 94720, USA*
[f] *Center for Geophysical Investigation of the Shallow Subsurface, Boise State University, Boise, ID 83725, USA*

ARTICLE INFO

Keywords:
Geothermal play fairway analysis
Snake River Plain
GIS
Common risk segment maps

ABSTRACT

The Snake River Plain (SRP) volcanic province overlies the track of the Yellowstone hotspot, a thermal anomaly that extends deep into the mantle. Most of the area is underlain by a basaltic volcanic province that overlies a mid-crustal intrusive complex, which in turn provides the long-term heat flux needed to sustain geothermal systems. Previous studies have identified several known geothermal resource areas within the SRP. For the geothermal study presented herein, our goals were to: (1) adapt the methodology of Play Fairway Analysis (PFA) for geothermal exploration to create a formal basis for its application to geothermal systems, (2) assemble relevant data for the SRP from publicly available and private sources, and (3) build a geothermal PFA model for the SRP and identify the most promising plays, using GIS-based software tools that are standard in the petroleum industry.

The study focused on identifying three critical resource parameters for exploitable hydrothermal systems in the SRP: heat source, reservoir and recharge permeability, and cap or seal. Data included in the compilation for heat source were heat flow, distribution and ages of volcanic vents, groundwater temperatures, thermal springs and wells, helium isotope anomalies, and reservoir temperatures estimated using geothermometry. Reservoir and recharge permeability was inferred from the analysis of stress orientations and magnitudes, post-Miocene faults, and subsurface structural lineaments based on magnetics and gravity data. Data for cap or seal included the distribution of impermeable lake sediments and clay-seal associated with hydrothermal alteration below the regional aquifer. These data were used to compile Common Risk Segment maps for *heat, permeability,* and *seal*, which were combined to create a Composite Common Risk Segment map for all southern Idaho that reflects the risk associated with geothermal resource exploration and identifies favorable resource tracks.

Our regional assessment indicated that undiscovered geothermal resources may be located in several areas of the SRP. Two of these areas, the western SRP and Camas Prairie, were selected for more detailed assessment, during which heat, permeability, and seal were evaluated using newly collected field data and smaller grid parameters to refine the location of potential resources. These higher resolution assessments illustrate the flexibility of our approach over a range of scales.

1. Introduction

The Snake River Plain (SRP) volcanic province overlies a thermal anomaly that extends deep into the mantle and represents one of the highest heat flow provinces in North America (*e.g.,* Blackwell and Richards, 2004). The Yellowstone hotspot continues to feed a magma

* Corresponding author.
E-mail address: john.shervais@usu.edu (J.W. Shervais).
[1] Current address: Geologica Geothermal Group, Inc, 9920 Pacific Heights Blvd, Suite 150, San Diego, CA 92121, USA.

https://doi.org/10.1016/j.geothermics.2023.102865
Received 28 March 2023; Received in revised form 30 October 2023; Accepted 31 October 2023
Available online 17 November 2023

system that underlies southern Idaho and has produced basaltic volcanism as young as 2000 years old (Kuntz et al., 1986a; Shervais et al., 2005). It has been estimated to host up to 855 MW of near-term potential geothermal power production, most of which is associated with the Snake River Plain volcanic province (Fleischmann, 2006). Additional resources reside in surrounding regions, tied to elevated heat flow associated with Basin and Range-type plays (*e.g.*, Welhan, 2016).

Play Fairway Analysis (PFA) is an approach to exploration pioneered by the petroleum industry that integrates data at the regional or basin scale (the *fairway*) to define favorable trends for exploration in a systematic fashion (*plays*). Data are integrated to highlight which plays have the highest likelihood of success (*prospects*). PFA provides greater technical rigor than traditional exploration approaches and facilitates quantitative, risk-based decisions even when data are sparse or incomplete (*e.g.*, Grant et al., 1996; Fugelli and Olsen, 2005). The goal of PFA is to minimize risk in exploration and to allow focus on areas with a higher probability of success.

PFA is a mature methodology in petroleum, but it is a new exploration technique for the geothermal industry. Past techniques were based on conceptual models of systems as a whole or targeted individual sites, and current exploration methodologies address those conceptual models (*e.g.,* Ward et al., 1981; Walker et al., 2005; Cumming, 2009). The geothermal industry has evolved from drilling hot spring occurrences to exploration of blind systems within known or inferred geothermal trends, and has identified distinct geothermal play types (*e.g.,* Moeck, 2014), but generally has not adopted PFA. A U.S. Department of Energy initiative funded over the last decade stimulated interest in this application (*e.g.,* Nielson and Shervais, 2014; Nielson et al., 2015; Shervais et al., 2017; Lautze et al., 2017a, 2017b; Ito et al., 2017) and represents a new approach that may aid in the discovery of buried or blind geothermal systems. A key challenge is to adapt this analysis in a way that provides meaningful results for a wide range of geothermal settings and measurable return on investment (Nielson et al., 2015).

Our goals for this study were to: (1) adapt PFA methodology for geothermal exploration to create a formal basis for its application to geothermal systems, (2) assemble relevant data for the SRP from publicly available and private sources, and (3) build a geothermal play fairway model for the SRP to identify the most promising plays using software tools we have developed from standards in the petroleum industry tailored to geothermal exploration. Our ultimate goals are to lower the risk and cost of geothermal exploration and to stimulate the exploration and development of new geothermal power resources in Idaho. Our approach to achieving these goals, including its application to a wide range of geothermal settings, is detailed in our companion paper (DeAngelo et al., this volume). Acronyms and abbreviations are listed in Table 1.

The success of PFA in geothermal exploration depends on defining a systematic methodology that is grounded in theory (as developed within the petroleum industry over at least three decades) and the geologic and hydrologic framework of real geothermal systems. The SRP PFA project has contributed to the development of this approach by cataloging the critical parameters of exploitable hydrothermal systems and establishing risk matrices that evaluate these parameters in terms of both *probability of success* and *level of knowledge*. These matrices were used as guidelines to construct an approach using Arc®GIS (ESRI, 2023) that allowed us to compile a range of data types with distinct characteristics and confidence values, and to process them in a consistent and systematic fashion across the entire study area. GIS has been used in geothermal exploration previously (*e.g.,* Prol-Ledesma, R.M., 2000, Noorollahi et al., 2008; Trumpy et al., 2015; Dezayes et al., 2022), but not within the context of play fairway analysis.

The study area encompasses almost all of southern Idaho, spanning 6° of longitude (~500 km EW) and over 2.5° of latitude (~300 km NS), or about 150,000 km^2 (Fig. 1). Most of the study area is underlain by a basaltic volcanic province that overlies a mid-crustal intrusive complex, which in turn provides the long-term heat flux needed to sustain geothermal systems (Shervais et al., 2006; Nielson and Shervais, 2014). The area represents a new conceptual model for geothermal systems, one that includes aspects of volcano-hosted systems and structurally controlled Basin and Range systems.

Table 1
Abbreviations used in the text.

Abbreviation	Refers to
AFB	Air Force Base
Arc®GIS	Software used for geographic analysis
BLM	Bureau of Land Management
CCRS	*Composite Common Risk Segment* map
CRS	*Common Risk Segment* maps
DOD	Department of Defense
DOE	Department of Energy
EM	Electromagnetic, including resistivity
GIS	Geographic Information System
GPS	Global Positioning System
GTO	Geothermal Technologies Office
IDWR	Idaho Department of Water Resources
IGS	Idaho Geological Survey
INL	Idaho National Laboratory
KGRA	Known Geothermal Resource Area
LBNL	Lawrence Berkeley National Laboratory
MT	Magnetotellurics
NFS	National Forest Service
NGDS	National Geothermal Data System
NREL	National Renewable Energy Laboratory
PACES	Pan-American Center for Earth and Environmental Studies
PFA	Play Fairway Analysis
R/Ra	$^3He/^4He$ isotopic ratio relative to atmospheric
RASA	Regional Aquifer Study Area
SRP	Snake River Plain
ESRP, WSRP, CSRP	Eastern, Western, Central SRP
SMU	Southern Methodist University Geothermal Laboratory
SRRA	Snake River Regional Aquifer
T_S, T_D	Stress analysis: slip tendency, dilation tendency
USGS	U.S. Geological Survey

2. Play fairway analysis concept adapted to geothermal exploration

The fundamental parameters required for petroleum plays are source rocks, reservoir rocks, migration pathways, and seals (Shell Exploration and Production, 2013; Neber et al., 2012). To be considered a prospect, plays must also contain structural or stratigraphic traps, and have a thermal history conducive to hydrocarbon generation at a time when all the other required elements (*e.g.*, reservoirs, pathways, seals, traps) were in place. Petroleum fairway analysis begins at the basin scale, progressively focuses in on the play scale, and finally to the prospect scale. Our challenge was to adapt this methodology to geothermal systems in a way that preserves the fundamental strengths of the scientific approach and risk-based aspects developed by the petroleum industry, but which makes sense for geothermal systems.

In this section, we correlate the fundamental parameters required for petroleum plays with their equivalent parameters in geothermal systems based on the conceptual model of Nielson and Shervais (2014). This model envisages a hybrid of the structurally controlled Great Basin geothermal system, and volcanically driven systems. Thermal energy is provided by a basaltic mid-crustal intrusive complex of basaltic sills and overlying shallow subvolcanic reservoirs, whereas fault systems form hydrothermal reservoirs and conduits for recharge (Nielson and Shervais, 2014; Nielson et al., 2017; Shervais et al., 2018). Heat flux is maintained by continued injection of new magma into the sill complex and this heat is preserved by a seal that both insulates the reservoirs and prevents venting to the surface (Nielson et al., 2017).

2.1. Heat (source)

A proximal heat source is the principal requirement for a high-

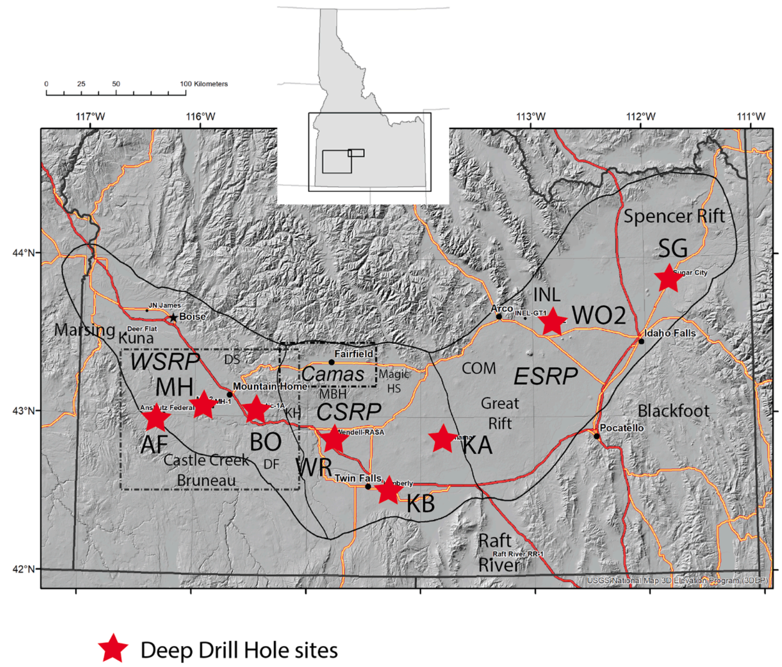

Fig. 1. Location map of the Snake River Plain study area (outlined in black) in southern Idaho. Western, Central, and Eastern SRP regions are outlined in black and labelled in italic (*WSRP, CSRP, ESRP*). Interstate highways shown in red, other major highways in yellow. Features indicated include (in the ESRP): Craters of the Moon (COM), the Great Rift, the Spencer Rift Zone, and the Idaho National Laboratory (INL), along with deep drill holes WO-2; in the CSRP: the Kimama, Kimberly, and Wendell-RASA deep drill holes, the Mount Bennett Hills (MBH), Magic Hot Springs, and King Hill (KH); in the WSRP: the Bostic-1A, Anshutz-Federal, Deer Flat, JN James and Mountain Home AFB (MH-1, MH-2) deep drill holes, the Castle Creek-Bruneau thermal area, and the Marsing and Kuna Butte areas. Dashed squares outline focus areas shown in Figs. 7 and 8. Hillshade from USGS 3D Elevation Program (U.S. Geological Survey, 2019).

temperature geothermal system that is within economically accessible drilling depths. The SRP is one of the highest heat flow provinces in North America and is associated with extensive Pliocene-Pleistocene volcanism (Blackwell, 1989, 1992). Within that province, we looked for areas where temperatures are enhanced by repeated or high-level magmatism. Using the Mountain Home core hole MH-2 as an example, there are hydrothermal breccias likely formed at temperatures >350 °C that indicate proximity to an intrusive body (Nielson et al., 2012) as well as fluid inclusion data that indicate past water temperatures of 186–368 °C (Atkinson et al., 2017).

In order to identify areas underlain by these complexes and associated heat sources, we used a wide range of geological, geochemical, and geophysical data including: regional heat flow data; the age, size, and density distribution of volcanic vents; gravity and magnetic field data; magnetotellurics (MT); seismic surveys; groundwater temperatures; and estimates of deep reservoir temperatures derived from isotopic, cation, and multicomponent geothermometers (*e.g.,* Neupane et al., 2014; Cannon et al., 2014). Helium isotopic values were also utilized in a supporting role to identify fluids that contain He with a significant mantle component (R/Ra > 1.5) (Dobson et al., 2015). Rhyolite domes and lavas are less common (*e.g.*, Big Southern Butte), but may also form an important heat source if they are underlain by relatively shallow magma chambers. In some areas, heat appears to come from deep circulation within the crust (*e.g.*, Twin Falls area).

2.2. *Permeability (reservoir)*

Geothermal reservoirs are almost exclusively reliant on fracture permeability associated with fracturing due to tectonic and magmatic processes (*e.g.,* Grant and Bixley, 2011). Surface exposures of bedrock are amenable to mapping of structural features such as faults and lineaments, but in many settings, sedimentary basins adjacent to topographic highs mask evidence of bedrock faulting and surface ruptures typically degrade quickly. In addition, the presence of extensive, young volcanic lava flows obscures older faults in the subsurface.

Fractures are difficult to characterize in the subsurface, but their presence can be predicted by steep gravity gradients, alignment of volcanic vents, petrophysical analyses of wireline log data, and an understanding of the relationships between lithology, lithostratigraphy, and mechanical properties. Analysis of fault trace maps and quantitative structure/stress analysis (slip tendency [T_S]and dilation tendency [T_D]) was used to help locate permeability associated with large, mapped structures (*e.g.,* Siler et al., 2016). Permeability conducive to geothermal systems is typically highest within step-overs (transfer zones), accommodation zones, and fault intersections (*e.g.,* Faulds et al., 2013) and these are high priority targets for identification and mapping. MT and magnetics provide information for identifying zones of alteration produced by interaction of geothermal fluids with the host rock. Geothermal reservoirs also discharge fluids that are often detectable by fluid geochemical methods, enhanced groundwater temperatures, or hot springs and other surface manifestations. The existence of thermal features highlights the presence of permeable flow paths through which thermal waters migrated up to the surface.

2.3. *Permeability (Migration pathways, recharge)*

Recharge by the migration of water into the geothermal system is critical to maintaining a long-lived resource. The hydrology of the SRP is complex. In the central-eastern SRP, the upper parts of the Snake River Regional Aquifer (SRRA) are reasonably well known around the Idaho National Laboratory site (*e.g.,* Welhan et al., 2002); however, the deeper parts are understood only from deep holes, such as the Kimama hole drilled during Project Hotspot (Lachmar et al., 2017; Potter et al., 2018, 2019), and from electromagnetic (EM) and MT data (Whitehead, 1986; Lewis and Young, 1989; Lindholm, 1996). Deep groundwater circulation is less constrained in the western SRP, where lake sediments dominate and deep drill holes are rare (*e.g.*, Bostic 1-A well: Arney, 1982; Mountain Home AFB wells: Lewis and Stone, 1988; Lachmar et al., 2019). In all areas, evidence for deep groundwater circulation is found in hot springs and thermal wells characterized by low $^3He/^4He$ ratios (<0.1), which shows that deep magmatic sources and mantle constituents are not involved (Neupane et al., 2014). Important recharge paths are provided by tectonic faulting that allow fluids to penetrate beneath lake beds and into geothermal reservoirs (*e.g.,* Sibson, 1994, 1996). As a result, we consider migration pathways in concert with reservoir permeability.

2.4. Seal

An impermeable seal is a common feature of many geothermal systems (Facca and Tonani, 1967), and is often seen as a critical feature for the preservation of an active geothermal system. In the absence of a seal, thermal fluids will escape to form surface hot springs (and accentuate heat release to the surface via advective heat transfer) or will mix with cold waters in shallower aquifers. Overlying sediments, which have lower thermal conductivities than the volcanic reservoir rocks, also act as a thermal blanket to retain heat. Project Hotspot demonstrated that lake sediments, hyaloclastites (glassy volcanic sediments), and altered basalts all may serve as effective reservoir seals in the SRP region (Shervais et al., 2013; Nielson and Shervais, 2014). The distribution of lake sediments in the SRP is documented by surface exposure and well logs. In addition, detailed studies of core from deep drill holes in the eastern SRP show that the base of the regional SRP aquifer is marked by pervasive clay alteration in the basalt groundmass, as well as a shift from convective geotherms (within the aquifer) to conductive geotherms (below the aquifer) (*e.g.,* Morse and McCurry, 2002; Shervais et al., 2013; Lachmar et al., 2017). Thus, the base of the aquifer defines the top of a regionally significant impermeable seal within the basalts. The depth to hydrothermally altered basalts and hyaloclastites, which define the depth to the base of the aquifer in the ESRP, may be mapped using electrical resistivity. The distribution of this aquifer has been documented by Whitehead (1986) and Lindholm (1996) using resistivity surveys and well data.

3. Methodology

We analyze direct and indirect indicators of geothermal potential to characterize the three critical geothermal resource components: *heat source, permeability,* and *seal* (Nielson et al., 2015). The SRP was divided into three main regions based on tectonic and volcanic setting, which differ in their stratigraphy and structure. The main regions are (1) the eastern SRP, including Craters of the Moon-Great Rift along its western margin, (2) the central SRP, comprising the axial portion of the plain between Craters of the Moon-Great Rift on the east and Hagerman-Bliss on the west, as well as the Bruneau-Jarbidge eruptive center (Bonnichsen 1982), the Mount Bennett Hills, and the Camas Prairie, and (3) the western SRP graben and adjacent regions (Fig. 1). Subregions comprising areas of interest adjacent to the margins of the plain include Basin and Range areas north and south of the ESRP; the Idaho Batholith (Taubeneck, 1971), which lies largely north of the WSRP and CSRP; and the Owyhee Plateau (*e.g.*, Manly, 1996), which lies south of the WSRP.

A *resource attribute worksheet* was created to summarize important properties (heat, permeability, seal) and the types of data needed to identify them (*e.g.,* heat flow, volcanic vents, faults, gravity and magnetic lineations, *etc.*). The resource attribute worksheet also included data sources and links where known (*supplemental file S1*). Critical element risk matrices were produced for attributes that assess model favorability against data confidence or assess an attribute for model favorability. The primary foci for these risk matrices are heat source and reservoir quality (permeability). The critical element risk matrices were based in part on the resource attribute worksheet, which defined many of the critical elements of source, reservoir, and seal; and in part on our evaluation of the uncertainty expected within each data type. Reservoir seal is relatively simple, because it consists of either impermeable sediments, whose distribution is relatively well known, or alteration self-seal, which is difficult to predict but may be inferred from resistivity studies (*e.g.,* Whitehead, 1986; Lindholm, 1996).

Raw data were converted into ArcGIS shapefiles (*data layers*), with multiple *data layers* for each component. These *data layers* were processed into two-dimensional grid surfaces, or *evidence layers*, typically using either interpolation (estimating a continuous attribute using data measured at finite locations, *e.g.,* heat flow) or as density functions (for discontinuous data converted into a continuous function). Because different data types have different uncertainties associated with their collection, each *evidence layer* has its own *confidence layer*, which reflects geographic variations in these uncertainties. *Risk maps* represent the product of *evidence* and *confidence layers* and are the basic building blocks used to construct *Common Risk Segment (CRS)* maps for *Heat, Permeability*, and *Seal.* In a final step, these three maps were combined into a *Composite Common Risk Segment (CCRS)* map for analysis of undiscovered geothermal resources. The CCRS map identifies several priority targets for future, focused study. The workflow for this process is shown in Fig. 2, and a detailed description of our methodology is presented in a companion paper (*DeAngelo et al., this volume*).

Work was carried out in two phases (DeAngelo et al., 2016, 2021a, 2021b). Phase 1 was a regional study that encompassed all of southern Idaho south of 44.8° N latitude (Fig. 1), based entirely on published data and new data compilations. Phase 2 focused on more localized analysis of smaller regions: the western SRP and Camas Prairie (Fig. 1 insets). Phase 2 analyses generated finer-scale assessments of our previously compiled data, along with newly acquired geophysical and geologic data (*e.g.*, Shervais et al., 2017, 2018; Glen et al., 2017).

4. Phase 1: regional studies

4.1. Data compilation

Data were compiled from a range of public and private sources (Appendix A). The data collected include geologic maps at scales from 1:24,000 to 1:250,000; structural features (faults, lineaments); vent locations, ages, and types from geologic maps and other sources; heat flow from the U.S. Geological Survey (USGS) and Southern Methodist University (SMU) Geothermal Laboratory databases; groundwater temperatures from the USGS and Idaho Department of Water Resources (IDWR); aeromagnetic data; existing regional gravity data as well as newly collected high resolution profile data, and processed potential field (gravity and magnetic) data yielding subsurface structural interpretations, passive seismic velocity, magnetotelluric and crustal thickness data from *Earthscope*, regional EM data from USGS reports, the locations of 56 commercially-available active source seismic lines and other public domain seismic lines, distribution, thickness and age of lacustrine sediment seals, the distribution and temperatures of thermal springs and wells from IDWR and the National Geothermal Data System (NGDS), water chemistry and stable isotope chemistry from USGS and from partner GTO-funded projects, and He isotopes from partner GTO-funded projects. Data products are archived at https://gdr.openei.org/submissions/733 and https://gdr.openei.org/submissions/734.

4.1.1. Geologic maps

Geologic maps used for the project include those published by the USGS and Idaho Geological Survey (IGS) and maps published in journals. Most of the SRP and adjacent areas are covered by 1:100,000 1° sheets or 1:125,000 county maps, most of which are compiled from mapping done originally at 1:24,000 scale (7.5′ quadrangle) or in a few cases, 1:62,500 scale (15′ quadrangle). A few areas are represented by older 1:250,000 scale maps (2° sheets). A list of maps used in this compilation is presented in Appendix A.

4.1.2. Heat flow and thermal gradients

Heat flow and thermal gradient drillhole data were compiled from

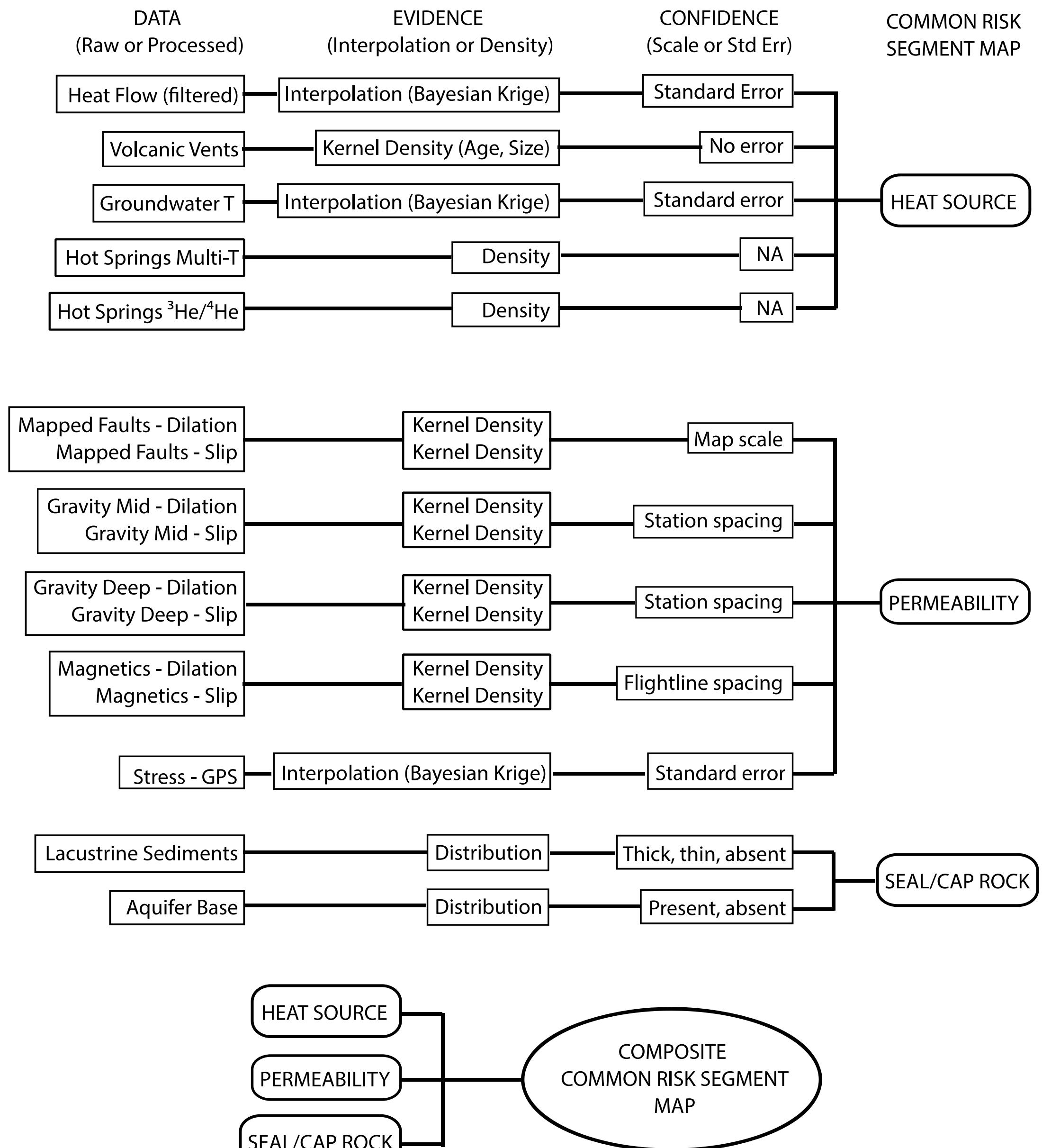

Fig. 2. Flowchart showing the GIS workflow for evaluating geothermal potential. Heat source, Permeability, and Seal indicators are grouped separately. Columns show the original data layers employed, the evidence layers processing protocols, and the confidence measures. Common Risk Segment (CRS) maps for Heat, Permeability, and Seal are combined into the Composite Common Risk Segment (CCRS) map for final analysis. T = temperature. Derivation of confidence layers is discussed in the companion paper DeAngelo et al. (this volume); NA indicates that data density is too sparse to calculate a confidence value.

USGS and SMU Geothermal Lab databases (*e.g.,* Williams and DeAngelo, 2008;2011; Blackwell, 1989; Blackwell and Richards, 2004), as well as data from the National Geothermal Data System (Fig. 3A). Heat flow data are not evenly distributed, with the highest density of measurements found in the WSRP and across the border in eastern-most Oregon. Thermal gradient wells in the eastern SRP are clustered at the Idaho National Laboratory (INL) site and along the eastern edge of the plain near Island Park caldera, with scattered coverage elsewhere. Large data gaps are found in the axial region from Idaho Falls to Hagerman (on the western edge of the Central SRP (CSRP)). These gaps correspond largely to the distribution of the Snake River aquifer, which renders measurement of conductive thermal gradients impossible in all but the deepest wells (*e.g.,* Williams and DeAngelo, 2011; McLing et al., 2016). Further, if thermal gradients are estimated from bottom hole temperatures and surface temperatures, the resulting gradient will give erroneously low heat flow. We have used data on aquifer distribution and thickness to correct for this effect where possible, both in the Snake River aquifer system and in the smaller but still important system on the Mountain Home plateau. In addition, new heat flow data from two Project Hotspot wells and one older well provide important new control points (Lachmar et al., 2017; Lachmar et al., 2019).

Groundwater temperature reflects thermal flux from below. Groundwater temperatures (measured in water supply wells) and surface flow from the mountains of eastern Idaho and Wyoming are characterized by temperatures ~8 °C, which represents the baseline temperature of the Snake River aquifer in the eastern and CSRP. Groundwater temperatures increase gradually from NE to SW in this region in response to thermal flux from below the aquifer (*e.g.,* Blackwell et al., 1992; Smith, 2004; McLing et al., 2014, 2016). Further, groundwater temperatures are uniformly high in the WSRP due to the thick insulating layer of lacustrine sediments. Because groundwater temperatures respond well to the underlying heat flux, they can be used

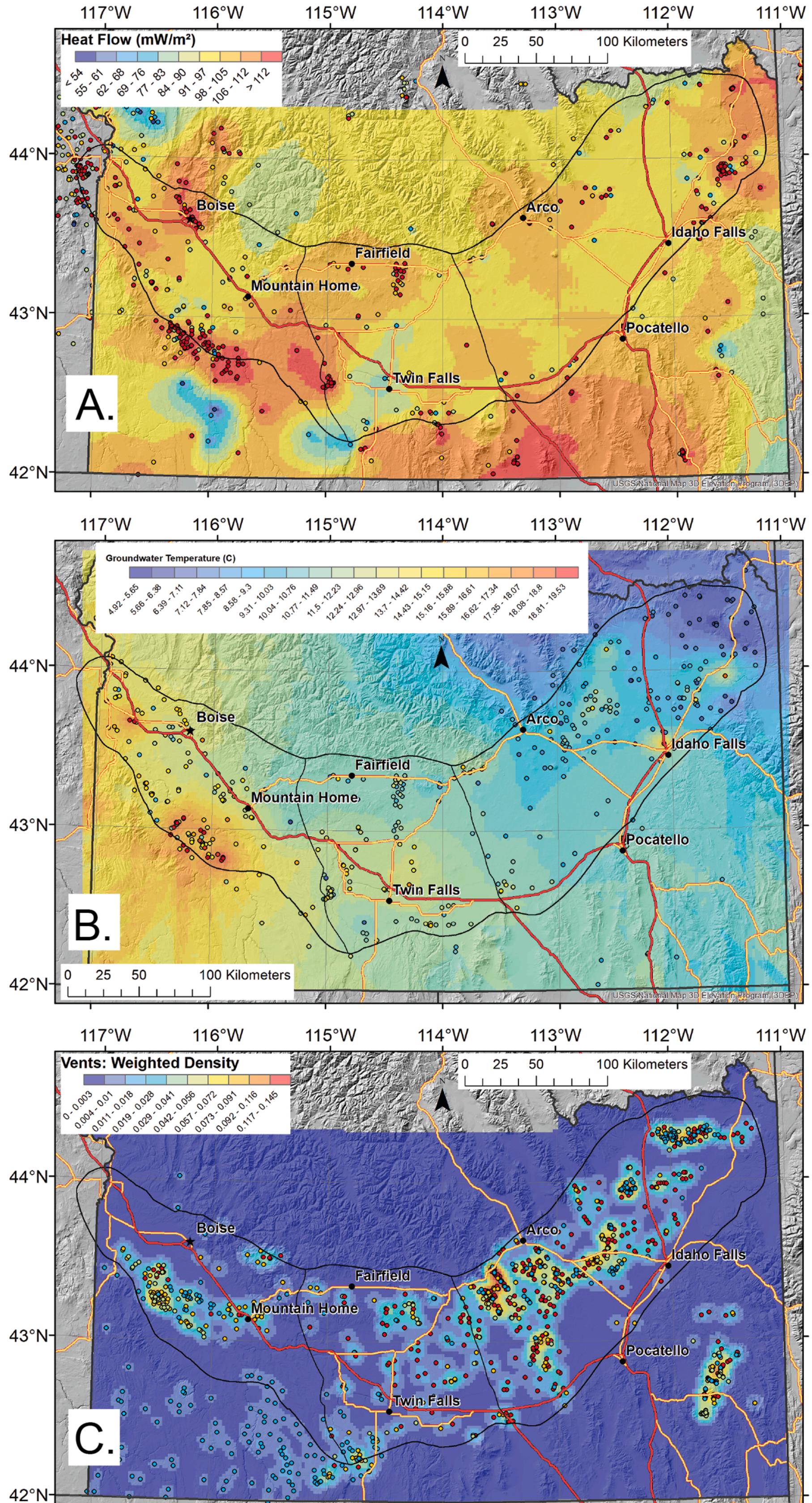

(caption on next page)

Fig. 3. Examples of evidence layers used to compile CRS maps for Heat. (A) Heat flow map showing the location of data points (wells with conductive thermal gradients and measured rock conductivities). The interpolated surface for heat flow is produced by empirical Bayesian Kriging, and its confidence layers from the standard error of the interpolated surface. (B) Groundwater temperature distribution showing data points. This map reflects the effect of underlying heat flow on groundwater temperatures but has a much higher primary data density due to the abundance of water wells and the fact that thermal gradients and conductivities are not needed to process. Note that overall groundwater temperatures increase from east to west; they are lowest in the ESRP and highest in the CSRP and WSRP. (C) Locations of volcanic vents, superimposed on a kernel density function of their distribution (weighted for size and age). Volcanic vents are more common in the ESRP where young volcanism dominates, but high vent densities are also seen in the Blackfoot area of SE Idaho, and in parts of the WSRP. A density surface for volcanic vents was calculated using a kernel density function within ArcGIS (see DeAngelo et al., this volume). Hillshade from USGS 3D Elevation Program (U.S. Geological Survey, 2019).

as a proxy for heat flux to supplement the more limited heat flow database (Fig. 3B).

4.1.3. Volcanic activity

Areas with high concentrations of young volcanic vents are likely to overlie magma chambers or recent sill intrusions, making them a proxy for magmatic heat centers in the crust. Vent locations for basalts and rhyolites were compiled from a range of sources and cross-checked against topographic features and geologic maps for accuracy and completeness (Fig. 3C). Radiometric ages, though rare, were compiled where available, and all vents were classified by age using radiometric ages, magnetic polarity, or stratigraphic relations from geologic maps. Basalt vents were binned into six age groups ranging from Holocene to Miocene and older (see Appendix A). To correct for age-related degradation of small vents (*e.g.*, cinder and spatter cones), which are overrepresented in young volcanic fields, a size factor was assigned to each vent ranging from 0.1 for small cinder or spatter vents to 1.0 for shield volcanoes.

4.1.4. Geophysical data

Geophysical data used in this study included gravity and magnetic potential fields, resistivity, MT, and regional stress data compiled by the USGS, including high-resolution gravity and magnetic data produced by Project Hotspot (Shervais et al., 2014) and the distribution of subsurface lineaments derived from maximum horizontal gradients in gravity and magnetic data. Crustal-scale seismic profiling data (refraction and receiver function analyses) and earthquake seismic data (NEIC and INL) from southern Idaho were also compiled. These datasets include seismic profiles published across the WSRP by Hill and Pakiser (1967) and by Sparlin et al. (1982), Peng and Humphreys (1998), and DeNosaquo et al. (2009) for the ESRP. USArray (Earthscope) seismic and MT results provide the lithospheric framework, crustal thickness, and identify highly conductive regions beneath southern Idaho (*e.g.,* Smith et al., 2009; Gao et al., 2011; Kelbert et al., 2012).

Gravity data from Project Hotspot (1866 new gravity stations) were combined with gravity data from the surrounding areas (including parts of ID, OR, NV, UT, WY and MT) and downloaded from the PACES data portal (Starks et al., 1997). Existing data provided regional coverage between detailed high-resolution gravity profiles and to extend profiles beyond the plain. The regional magnetic grid used in this report was derived from the Magnetic Anomaly Map of North America (Bankey et al., 2002). We have also used a higher resolution grid for the State of Idaho (McCafferty et al., 1999). Additional datasets integrated into our analyses include geodetic results from Payne et al. (2013) and local MT and resistivity survey results. These surveys, summarized by Stanley et al. (1977) across the ESRP and Whitehead (1986, 1992) across the SRP, have provided the framework for resistive sedimentary basin geometries and more conductive aquitards that may cap blind geothermal systems.

4.1.5. Stress and strain

Faulds et al. (2013) have shown that most productive hydrothermal resources in the Great Basin occur in complex fault interaction zones that have dilation and slip components that result in open fractures along some part of the fault. In order to assess the impact of stress and strain to reservoir favorability, we have applied standard methods for assessing the effects of stress and strain to our study area. These calculations were applied to each segment in a digitized fault or lineament, and the results were used to weight that segment in the kernel density functions described above. Regional stress fields were compiled from GPS measurements (Payne et al., 2008, 2012) and well bore breakouts (*e.g.,* Kessler et al., 2017).

Critically stressed fault segments have a relatively high likelihood of acting as fluid flow conduits (Zoback and Townend, 2001; Ito and Zoback, 2000; Townend and Zoback, 2000; Barton et al., 1995, 1998; Morris et al., 1996; Sibson, 1994). As such, the tendency of a fault segment to slip (slip tendency; T_s) (Morris et al., 1996) or to dilate (dilation tendency; T_d) (Ferrill et al., 1999) provides a quantitative indication of the likelihood of a certain fault segment to be critically stressed, for either slip or dilation, relative to another fault segment. The slip tendency of a surface is defined by the ratio of shear stress to normal stress on that surface (Morris et al., 1996):

$$T_s = \tau / \sigma_n.$$

Dilation tendency is defined by the stresses acting normal to a given surface (Ferrill et al., 1999):

$$T_D = (\sigma_1 - \sigma_n) / (\sigma_1 - \sigma_3),$$

where τ is the resolved shear stress on the fault plane, σ_n is the resolved normal stress on the fault plane, σ_1 the magnitude of the minimum stress, and σ_3 is the magnitude of the maximum stress. Slip and dilation tendency are both unitless ratios of the resolved stresses applied to the fault plane by ambient stress conditions. Values range from a maximum of 1, a fault plane ideally oriented to slip or dilate under ambient stress conditions to zero, a fault plane with no potential to slip or dilate. Slip and dilation tendency values were calculated for each fault segment and each discrete magnetic and gravity lineation in the focus study area. Because dip is not well constrained or unknown for many faults mapped within the study area, fault dip was assumed to be 70° for all faults (Siler et al., 2016). Magnetic and gravity lineations are assumed to be vertical. The resulting along-fault and fault-to-fault variation in slip or dilation potential is a proxy for along fault and fault-to-fault variation in permeability or fluid flow potential.

4.1.6. Faults and lineaments

Faults and lineaments were compiled largely from two sources: (1) USGS Quaternary fault database (Machette et al., 2003), and (2) Idaho Geological Survey database of Miocene and younger faults (Breckenridge et al., 2003). Additional faults were compiled from geologic maps and reports. The Idaho Geological Survey (IGS) database is more extensive but contains less information, so where duplicate records occur the USGS record was retained and the IGS record discarded. Individual fault strands are digitized into numerous short segments, each of which is considered a separate fault segment during data processing (*e.g.*, density counts). All fault segments are evaluated for slip and dilation tendency within the regional stress field, as discussed in Section 4.1.5, and these tendency values (0–1.0) are used as weights in the density functions (Fig. 4A).

In addition to mapped surface faults, we also digitized subsurface lineaments from maximum horizontal gradients in gravity and magnetic anomalies (Section 4.1.4). These lineaments are interpreted to represent

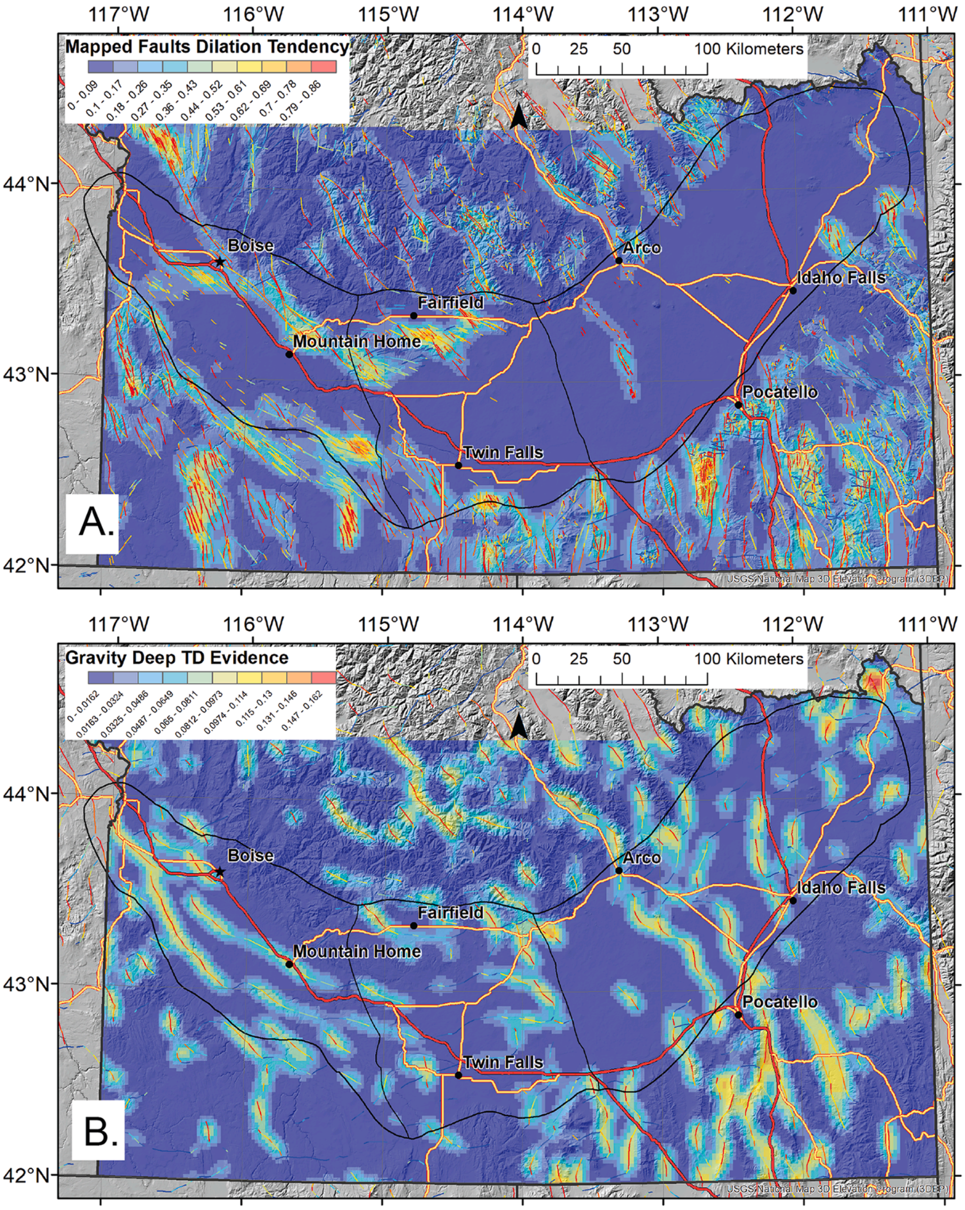

Fig. 4. Examples of evidence layers used to compile CRS maps for Permeability. (A) Mapped surface faults weighted for dilation tendency, color coded with hotter colors indicating higher dilation tendency (see text). Volcanic rift zones of the Great Rift are included with the faults. (B) Lineaments digitized from maximum horizontal gradients in deep gravity data, thought to reflect offsets in basement lithologies. The lineaments are weighted by dilation tendency and a density surface calculated using a kernel density function within ArcGIS (see DeAngelo et al., this volume). Hillshade from USGS 3D Elevation Program (U.S. Geological Survey, 2019).

major structural discontinuities in the subsurface. These data are crucial for most of the SRP because exposed faults are rare within the plain, but these structures are known to host geothermal permeability at depth (*e.g.,* Shervais et al., 2014). As with the mapped surface faults, these lineaments are evaluated for slip and dilation tendency within the regional stress field, and these tendency values are used to weight the density functions (Fig. 4B).

4.1.7. *Geochemistry of thermal waters*

Measured temperatures, geochemistry, and geothermometry of geothermal wells and thermal spring waters were obtained from USGS, IGS, and NGDS databases, as well as from ongoing studies being carried on by researchers at INL, the University of Idaho, and Lawrence Berkeley National Laboratory (LBNL) (*e.g.,* Young and Mitchell, 1973; McLing et al., 2002; Cannon et al., 2014; Neupane et al., 2014; Dobson et al., 2015). These data include results from recently developed multicomponent geothermometers as well as traditional cation methods (*e.g.,* Spycher et al., 2014; Palmer et al., 2014; Neupane et al., 2014) and compiled He isotope data (Dobson et al., 2015).

4.1.8. *Aquifer systems*

The SRP is characterized by major aquifer systems that can have a significant impact on heat flow measurements and on the depth needed to achieve sufficiently high temperatures for power production. Data for the distribution, thickness, and impact of these aquifers are obtained largely from publications of the USGS and the Idaho Department of Water Resources: Whitehead (1986); Whitehead and Lindholm (1985); Lindholm (1996); Whitehead (1992); Garabedian (1992); Newton (1991); Wood and Anderson (1981); Smith (2004).

The Snake River Regional aquifer system of the eastern and central SRP is the most substantial aquifer in the study area (Fig. 5A). This system is fed by inflow from the Big and Little Lost Rivers, Birch Creek,

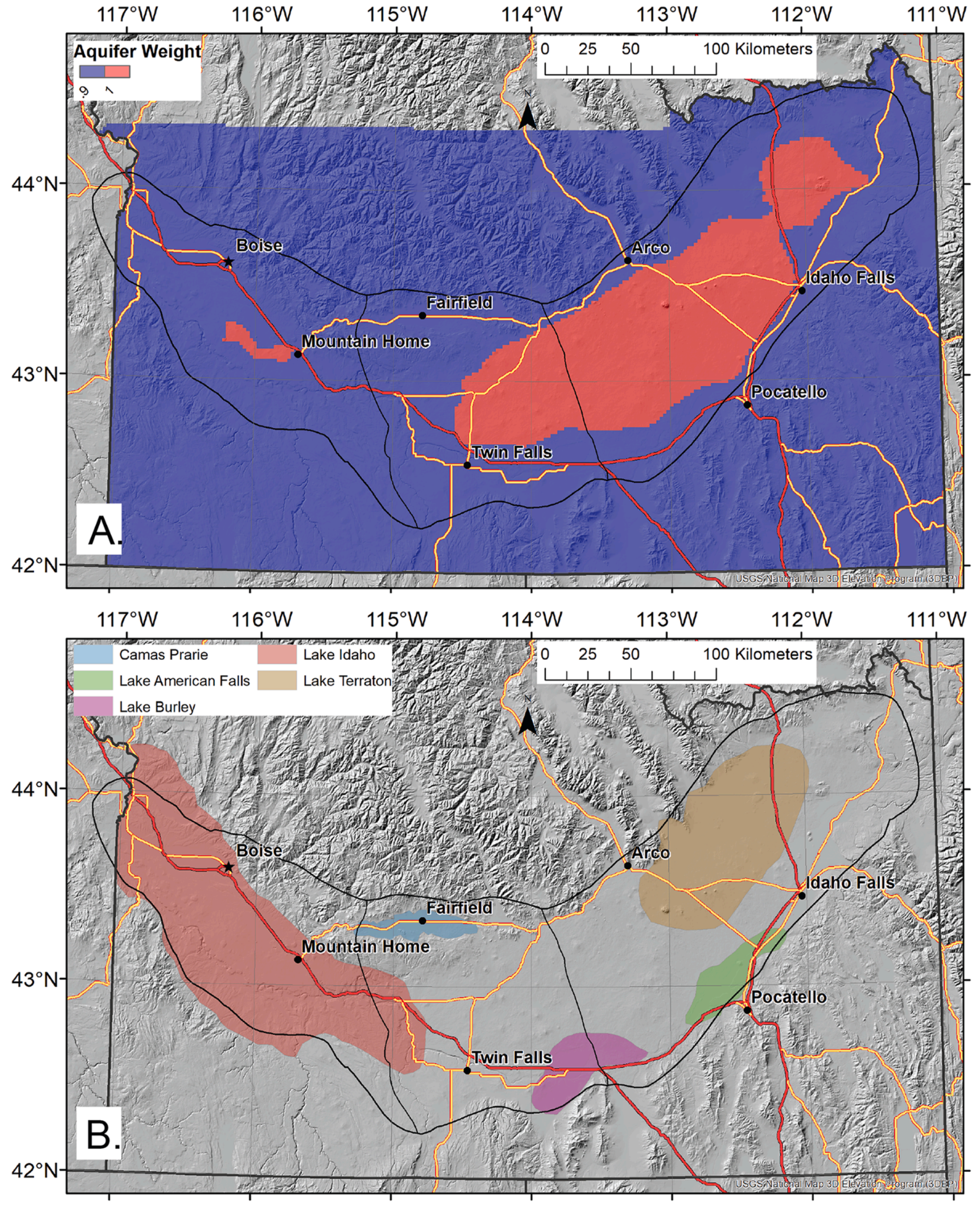

Fig. 5. Examples of evidence layers used to compile CRS maps for seal. (A) The distribution of major aquifers, whose lower boundary represents a seal formed by hydrothermal alteration of the deeper volcanic rocks. This seal is weighted either 1 (present) or zero (absent). (B) Distribution of paleolake sediments that form aquitards due to their fine grain size and lack of permeability. These are weighted by average thickness of the sediment layers, as discussed in the text. Hillshade from USGS 3D Elevation Program (U.S. Geological Survey, 2019).

and Henrys Fork river, and it emerges in a series of spectacular springs in the Thousand Springs-Hagerman area, 200–300 km SW of its recharge areas. Deep wells show that the aquifer extends to depths of 200–550 m in the ESRP and 980 m in the CSRP. The base of the aquifer is defined by the change from convective, nearly isothermal gradients within the aquifer, to conductive gradients below (Smith, 2004; McLing et al., 2016). The distribution and thickness of this aquifer has been delineated from electrical resistivity and well data by Lindholm (1996) and Whitehead (1992). The base of the regional aquifer represents the onset of clay alteration in the basalt groundmass, which forms an effective seal to the influx and escape of water or geothermal fluids (Sant, 2012).

The Snake River Regional aquifer is bounded on its southern and western margins by the Snake River canyon. Local aquifers, such as the Twin Falls low-temperature geothermal aquifer system, flow towards the Snake River from mountain ranges in the south (Street and DeTar, 1987; Garabedian, 1992; Lindholm, 1996; Whitehead, 1992).

In the WSRP, aquifers are limited by the distribution of impermeable lacustrine sedimentary rocks and surface drainages include the Bruneau, Jarbidge, Owyhee, and Boise Rivers, as well as the Snake. Gravel deposits comprise shallow aquifers in the Boise area and a perched aquifer in the Mountain Home area. The plateau between Boise and Mountain Home is capped by up to 300 m of basalt that hosts localized aquifers. These basalts are underlain by impermeable lacustrine sediments (Newton, 1991; Wood 1994; Wood and Clemens, 2002).

4.1.9. Distribution of lake sediments

Impermeable lacustrine sediments form regional and local aquitards that may confine aquifer systems and act as effective seals for geothermal systems. Sediments associated with paleo-Lake Idaho cover most of the WSRP with a minimum thickness of > 1 km, as recorded in drill core (Shervais et al., 2014; Wood and Clemens, 2002).

In the central and eastern SRP, lacustrine sediments are associated with five paleolake deposits: paleo-Lake Burley, paleo-Lake American Falls, paleo-Lake Terreton, and lake deposits that fill the valley of Camas

Prairie (Fig. 5B). The sediment layers in these are typically a few tens of meters to a few hundred meters thick, as documented by water wells and test wells (*e.g.*, Anderson et al., 1996, 1997; Desborough et al., 1989). Weights for the effectiveness of seal were assigned based on sediment thickness, ranging from 1.0 for paleo-Lake Idaho to 0.9 for paleo-Lake Terreton (note: data for Lake Terreton were added during Phase 2 of this study).

4.1.10. Lithologic and wireline logs from deep wells

Lithologic and borehole geophysical logs were compiled for deep wells including test wells at the INL site, USGS water resource and geothermal test wells, passive geothermal wells (Boise, Twin Falls districts), and wildcat petroleum exploration wells. The most complete records are from Project Hotspot, which drilled deep (1.8 to 1.9 km deep) holes at three locations across the SRP (Shervais et al., 2014). These wells provided about 5300 m of core and a complete set of wireline logs for each drill hole. Other deep holes that provided more limited data (typically lithologic logs, but some with wireline logs and temperature data) include INEL-1 and WO-2 (1524 m) at the INL site, Sugar City (696 m) and Wendell-RASA (343 m) in the ESRP and CSRP, and MH-1 (1342 m), Bostic 1A (2743 m), JN James (4389 m), Champlin Petroleum Upper Deer Flat No. 11–19 (2750 m), and Anschutz Federal #1 (3391 m) in the WSRP (Doherty, 1979; McIntyre, 1979; Embree et al., 1978; Doherty et al., 1979; Arney et al., 1982; Whitehead and Lindholm, 1985; Hackett et al., 1994; Breckenridge et al., 2006; Jean et al., 2013). These data were used to constrain stratigraphic variation within the SRP but were not incorporated into the formal GIS analysis.

Most water wells in the central and eastern SRP are too shallow to reveal much information, but an exception to this is the Twin Falls Warm Water district, which contains many moderately deep wells (150 m to 670 m depth) that tap into a low-temperature geothermal aquifer at 37 °C to 42 °C, used for passive space heating (Neely, 1996). Because they are located along the southern margin of the CSRP, these wells typically penetrate basalt and bottom in rhyolite lavas or welded ash flow tuffs. These wells lie outside the basaltic Snake River aquifer and provide information on a distinct hydrologic system that lies largely south and west of the Snake River. Relatively shallow (≤250 m) well data from the Burley and American Falls area are important for establishing the extent and thickness of lacustrine sediments from paleo-Lake Burley and paleo-Lake American Falls, which represent the most important lake seals in the ESRP (Neal Farmer, IDWR, personal communication, 2010; Desborough et al., 1989; Phillips and Welhan, 2006, WM 2011). The distribution of lacustrine sediment seals is shown in Fig. 5, including seals due to Lake Idaho and the Camas Prairie basin.

4.1.11. Cadastral data

The Snake River Plain PFA study area encompasses a wide variety of political, land use, cultural, infrastructural, and environmental attributes. Cadastral data were assembled using the *Geothermal Prospector* mapping tool developed by NREL for the DOE Geothermal Technologies Office (Getman et al., 2015). *Geothermal Prospector* is designed to assist users in determining locations that are favorable to geothermal energy development. Key regional cadastral data layers include Political (Federal, State, Tribal lands), land ownership (private, BLM restricted, NFS restricted, DOD restricted, other restricted), environmental (areas of critical environmental concern, brownfields, BLM closed areas, National Forest Service closed areas, Wilderness areas and study areas, greater prairie chicken/sage grouse range), infrastructure (operating geothermal plants, developing geothermal projects, transmission corridors), and resource (*Known Geothermal Resource Areas:* KGRA).

4.2. Phase 1 results

4.2.1. Distribution of heat

The distribution of heat throughout the SRP volcanic province was assessed using heat flow, groundwater temperatures, the distribution of volcanic vents (weighted by age, size, and composition), measured temperatures of thermal waters from springs and wells, calculated classical and multicomponent geothermometry temperatures of thermal waters from springs and wells, and the distribution of high $^3He/^4He$ (indicative of mantle volatile contributions) in thermal waters. Heat flow and groundwater temperatures were interpolated using empirical Bayesian Kriging (DeAngelo et al., this volume). Multicomponent geothermometers indicate high reservoir temperatures for Banbury Hot Springs, hot springs along the margins of the Mount Bennett Hills and ESRP, as well as for artesian hydrothermal water from the deep well MH-2 (WSRP). Helium isotope data present a similar picture, with high $^3He/^4He$ ratios found in thermal waters from Camas Prairie, Banbury Hot Springs, Arco, and the Blackfoot area (Dobson et al., 2015).

The CRS map for heat source (Fig. 6A) highlights several areas with high thermal potential: (a) large portions of the WSRP, including the Boise thermal district; areas south and west of Boise (Marsing-Kuna area); the Mountain Home area (both the town and Air Force Base (AFB)); the Castle Creek-Bruneau KGRA; and part of Bruneau-Jarbidge eruptive center; (b) the CSRP, including the Camas Prairie-Mount Bennett Hills region, Magic Hot Springs, and the Banbury-Miracle Hot Springs area; and (c) the ESRP, including Craters of the Moon and Great Rift, the Arco area (adjacent to the INL FORGE site), and the Spencer-High Point rift (Kuntz et al., 2002; Iwahashi, 2010), which trends EW and intersects the margin of Island Park caldera. Estimated heat flow is relatively high in SE Idaho, coincident with Basin and Range structures, although the volcanic fields around Blackfoot are not as high as the Raft River area farther south. Heat flow is somewhat elevated in the southeastern part of the Idaho Batholith (90–100 mW/m^2), which supports a number of thermal springs and pools in the Salmon River drainage.

4.2.2. Distribution of permeability (Reservoir/recharge)

Reservoir and recharge permeability were assessed using the weighted sum of mapped faults, magnetic lineaments, upper to mid-crustal gravity lineaments, and deep crustal gravity lineaments, each weighted by both slip tendency and dilation tendency. Risk maps for the deepest lineaments are weighted more heavily than those for shallow (magnetic) or surface features (mapped faults), which reflects the difficulty in imaging deeper structures and their correlation with large structural offsets in the basement. It also reflects the fact that surface faults are mapped with great precision in some areas, resulting in high fault densities in places where there may be little structural offset. Faulds et al., (2013) have shown that most productive hydrothermal resources in the Great Basin occur in complex fault interaction zones that have a dilational component resulting in open fractures along some part of the fault (*i.e.*, accommodation zones, fault intersections, and step-overs). A proxy for fault and lineament intersections at the regional scale of this study is fault density, where high fault (or lineament) densities tend to favor multiple intersections.

Mapped faults are restricted to the margins of the SRP (due to the ubiquitous presence of young volcanic rocks in the plain that tend to obscure older structures), with high densities in three areas (outside of the Basin and Range regions). Buried structures and lineaments, defined by high horizontal gradients in the gravity and magnetic anomalies, suggest significant permeability along the northern and southern margins of a major gravity anomaly in the WSRP. The CRS map for permeability (Fig. 6B) highlights several highly favorable areas for the basaltic sill play-type: (a) the WSRP, where high permeability is predicted in linear trends sub-parallel to the WNW-trend of the western plain range front faults or to the oblique trend of the central gravity high; (b) the CSRP, where high permeability is found in the Camas Prairie-Mount Bennett Hills area, near Fairfield, Idaho; (c) the ESRP, focused largely on the Arco rift zone that extends northward up the Big Lost River valley and southward past Big Southern Butte; and (d) the Blackfoot-Gem Valley region of SE Idaho.

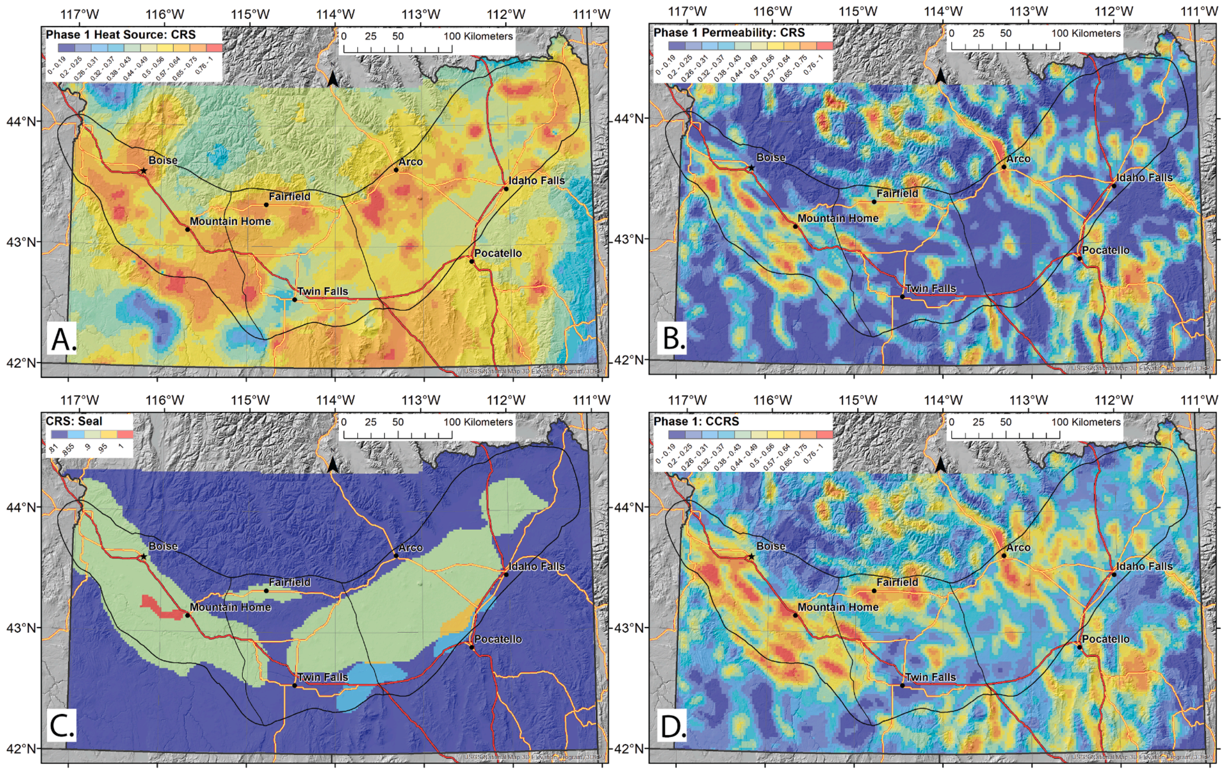

Fig. 6. Common Risk Segment (CRS) maps for (A) Heat, (B) Permeability, and (C) Seal, along with (D) the Composite CCRS map derived from these CRS maps. See text and DeAngelo et al., this volume, for discussion. Hillshade from USGS 3D Elevation Program (U.S. Geological Survey, 2019).

4.2.3. *Distribution of seals*

The SRP geothermal system has two potential seals: (a) fine-grained lacustrine sediments, which are largely impermeable and (b) self-seal of volcanic rocks by hydrothermal alteration (Nielson and Shervais, 2014). The first is relatively easy to map; the second much more difficult. The distribution of lake sediments is well known in the WSRP, where regional formations consisting largely of lacustrine sediments are widespread (*e.g.,* Bruneau, Glens Ferry, and Chalk Hills Formations; early Pleistocene, Pliocene, and Miocene in age). These formations were deposited by paleo-Lake Idaho, which filled the WSRP for much of its existence, and now provide an impermeable seal 0.5–1.6 km thick (Wood and Clemens, 2002). These formations gradually pinch out from west to east. Other sediment-filled basins include Camas Prairie (up to 500 m of sedimentary fill), the Burley area (up to 100 m of sediment), the American Falls area (10–30 m of sediment), and paleo-Lake Terreton, along the northern margin of the northeastern SRP (Neal Farmer, IDWR, written communication, 2010; Desborough et al., 1989; Phillips and Welhan, 2006, WM 2011; Anderson et al., 1996, 1997). For a lacustrine sedimentary seal to be effective, it must be relatively thick and continuous. Thus, paleo-Lake Idaho (WSRP) and the Camas Prairie basin have the most effective seals, paleo-Lake Burley is somewhat effective, and paleo-lakes American Falls and Terreton are considered relatively ineffective. Self-seal by alteration is difficult to ascertain without core data. The base of the Snake River aquifer is known to be controlled by the onset of clay alteration in basalt groundmass in response to previous hydrothermal alteration (Helm-Clark et al., 2004; Sant, 2012). Thus, we interpret the base of the regional and perched aquifers to represent the top of a hydrothermal seal that confines hydrothermal systems below it as well as the aquifer above.

The CRS map for seal (Fig. 6C) shows that the distribution of seal is extensive, with most areas having either significant thicknesses of lacustrine sediments (WSRP, Camas Prairie, Burley area) or a basal aquifer seal (ESRP). Hot springs located along the margins of the SRP show where the seal does not exist, or has been broached by faulting.

4.3. *Potential prospects: phase 1 assessment*

A preliminary assessment of plays and potential prospects based on our Phase 1 results suggests several areas where undiscovered geothermal resources may be found based on indicators of sufficient heat source and permeability below a sealed zone. In this section, we present an overview of geothermal potential within specific regions of the SRP and conclude with a discussion of the sites that have significant potential for exploitation. The following discussion is based on the CRS maps for Heat, Permeability, and Seal, and on the CCRS map that is a weighted sum of the heat CRS and permeability CRS times the seal CRS across the entire study area (Fig. 6A–D).

4.3.1. *Western Snake River Plain (WSRP)*

The WSRP presents numerous opportunities for geothermal exploration and was chosen for higher resolution assessment in Phase 2. It is characterized by relatively high heat, based on high groundwater temperatures and the extensive distribution of early to mid-Pleistocene basalt volcanoes, with some vents as young as ~200,000 years. Volcanic vents form clusters that follow the southern margin of the axial gravity high, and parallel the northern margin, with a dense cluster at its western end. The vent distribution corresponds to subsurface lineaments highlighted in the permeability CRS map, which combine to make an exploration target. The viability of these prospects is attested by Project Hotspot well MH-2, which was located on the southern margin of this gravity high and encountered hot (~150 °C) water at 1745 m depth in fractured basalt (Shervais et al., 2013, 2014; Lachmar et al., 2019). Thermal modeling (Garg et al., 2016) shows that this is a large regional thermal anomaly associated with multiple prospects.

4.3.2. *Central Snake River Plain (CSRP)*

The CSRP is characterized by a low density of young volcanic vents compared to the eastern SRP, but this is due in part to the older loess-covered surface of the vents here and to the rapid degradation of small cinder and spatter satellite vents that are common in the ESRP (Shervais et al., 2005). Basalt vents in the CSRP are typically 100 ka to 400 ka along the Axial Volcanic Zone, and older (up to 2–3 Ma) along the margins. However, the Holocene Shoshone lava field erupted from Black Butte Crater on the northern margin of the plain, just south of Magic Hot Springs, and other Holocene to late Pleistocene vents are found nearby in the Mount Bennett Hills (Kuntz et al., 1986b). Many of the vents in CSRP region are enormous, with diameters up to 20 km across and flow fields that extend 35–40 km from the vent (*e.g.,* Shervais et al., 2005). Deep heat flow is marginally higher than in the ESRP although shallow heat flow is still suppressed. Groundwater temperatures are markedly higher in the CSRP compared to the east, reflecting the effect of continuing heat flux from below as the aquifer waters move from their source in eastern Idaho to their outlets in the Thousand Springs area NW of Twin Falls.

Thermal resources are indicated by the presence of numerous hot springs throughout the region, typically along the margins of the plain (*e.g.,* the Banbury-Miracle HS area, the Magic Reservoir-Camas Prairie HS area, and Latty HS on the SW edge of the Mount Bennett Hills) and by the widespread warm water of the Twin Falls thermal district (Street and deTar, 1987; Street, 1990; Baker and Castelin, 1990). Thermal spring waters in the Banbury-Miracle, White Arrow (Mount Bennett Hills south-side), Latty (Mount Bennett Hills SW edge), and Magic Reservoir areas are characterized by high calculated equilibrium reservoir temperatures (~150–160 °C; Neupane et al., 2014). Thermal spring waters in the Banbury-Miracle, White Arrow, Camas Prairie, and Magic Reservoir areas are characterized by high $^3He/^4He$ ratios (R/Ra ≥1), high calculated equilibrium reservoir temperatures (~140–180 °C), and the presence of magmatic or hydrothermal methane (Dobson et al., 2015; Conrad et al., 2016; Neupane et al., 2017).

The central part of the Camas Prairie region is attractive and was also selected for more detailed assessment in Phase 2. It is cut by a through-going NW-trending fault system that divides NW-trending faults to the east from NE-trending faults to west, accounting for extensive fault intersections and hot springs that are distributed along these intersections, from the Camas Prairie into the Mount Bennett Hills to the south.

4.3.3. Eastern Snake River Plain (ESRP)

The ESRP is characterized by dense clusters of vents in the EW-trending Spencer-High Point rift and along the Axial Volcanic Zone (Iwahashi and Hughes, 2006; Iwahashi, 2010). Although there are some Holocene vents, most volcanic activity was late Pleistocene (Brunhes normal epoch, ≤780,000 years; Wetmore et al., 2009). The Axial Volcanic Zone contains three rhyolite domes (<700 ka) that postdate basalt, an older rhyolite cryptodome, and an evolved dacite volcano (Cedar Butte). There are two rhyolite cryptodomes on the southern margin (McCurry et al., 2008). As with the COM-Great Rift, deep heat flow is high, but heat flow based on shallow wells is much lower, and groundwater temperatures are low.

The Snake River Regional aquifer extends over much of the eastern SRP and masks the deeper geothermal resource (Smith, 2004; McLing et al., 2016); there is no surface faulting except along the margins, and there is little indication of buried permeability from gravity or magnetics. Payne et al., (2008, 2012) present GPS strain data that document extension in the Basin and Range regions north and south of the SRP, whereas the SRP itself moves as a coherent block with uniform velocity. This implies relative motion along the interface between the SRP and the adjoining mountain areas, but at this time there is no indication of faulting or earthquakes along these boundaries. Due to the effects of shallow groundwater flow, temperatures needed for electrical energy production are likely too deep to make these geothermal resources viable at this time.

4.3.4. Basin and Range Plays

There are two Basin and Range plays that may represent potential prospects (not counting the active Raft River site): the Arco Rift-Big Lost River Valley in central Idaho, and the Blackfoot-Gem Valley region of SE Idaho. The Blackfoot-Gem Valley region has been studied extensively by McCurry and colleagues (McCurry et al., 2011, 2015; McCurry and Welhan, 2012; Welhan et al., 2014; Welhan, 2016). A test well drilled by Unocal in the 1980s encountered a major flow of cold water moving towards Blackfoot reservoir (McCurry et al., 2011). However, a 3-km deep well drilled NE of the reservoir in 1979 by Conoco measured a bottom hole temperature of 190 °C, similar to the Bostic 1A well in the WSRP (Fleischmann, 2006). Welhan et al. (2014) and Welhan (2016) suggest that this resource comprises a large area with high heat flow (~100–220 mW/m^2) that is masked by structural relations in the SE Idaho fold and thrust belt.

5. Phase 2: local studies

Two regions were selected for more detailed assessment in Phase 2, the western SRP and the much smaller Camas Prairie area (Fig. 1 insets). Phase 2 assessments used the data compiled for Phase 1, along with newly acquired data, but employed higher resolution grid scales for generating data layers, fine-tuned weights used in compiling risk maps, and explored the effects of varying search radii on density functions (DeAngelo et al., this volume).

5.1. The WSRP fairway

The WSRP is an example of a regional fairway (as opposed to all southern Idaho, which comprises multiple fairways) that is largely a blind system because thermal features are only found along its margins (*e.g.*, the Boise Warm Water District; Fleischman, 2006). The WSRP fairway includes an area about 2° longitude x 2° latitude, which encompasses ~13,000 km^2. CCRS maps were constructed using a sampling grid of 500 m (*versus* 2 km in the regional, Phase 1 CCRS) with updated sample weights as discussed in DeAngelo et al. (this volume). Fig. 7 presents two versions of this CCRS in which the only difference is the diameter of the kernel density function search radius. The larger search radius (2.5 km, *versus* 10 km in the Phase 1 study) shows the general distribution of highly favorable areas (Fig. 7A, hotter colors). The smaller search radius (1 km) reveals specific lineaments defined largely by high gradients in the potential field anomalies (Fig. 7B). In both cases, the areas with highest favorability tend to lie along the margins of a well-defined gravity high that underlies the WSRP (Glen et al., 2017).

5.2. The Camas Prairie fairway

Camas Prairie is an example of a localized fairway that is less than one-quarter the size of the WSRP fairway (2000 km^2). It is a partially blind system with thermal features largely confined to the margins, but also extending part way into the basin. Faulting in the adjacent Mount Bennett Hills is thought to reflect stresses that underlie the Prairie as well. Subsurface faulting is defined by potential field gradients which highlight the EW-trending range front fault system and the NW-trending Pothole Fault system. Both systems are seen in Phase 2 CCRS maps which use Phase 2 weights and a sample grid of 100 m (Fig. 8). In Fig. 8A, the kernel density search radius is 2.5 km, whereas in Fig. 8B the radius is 1 km. The change in search radius highlights the subsurface lineaments, the most prominent being the Pothole Fault system, which extends NW across the Mount Bennett Hills and Camas Prairie. The area with highest potential for geothermal resources here is thought to be where the Pothole Fault system crosses the range front fault system.

6. Conclusions

The work presented here and in our companion paper (*DeAngelo et al., this volume*) demonstrates that the interpretive framework of PFA can be applied effectively to the systematic exploration of geothermal resources across a variety of tectonic settings. The incorporation of

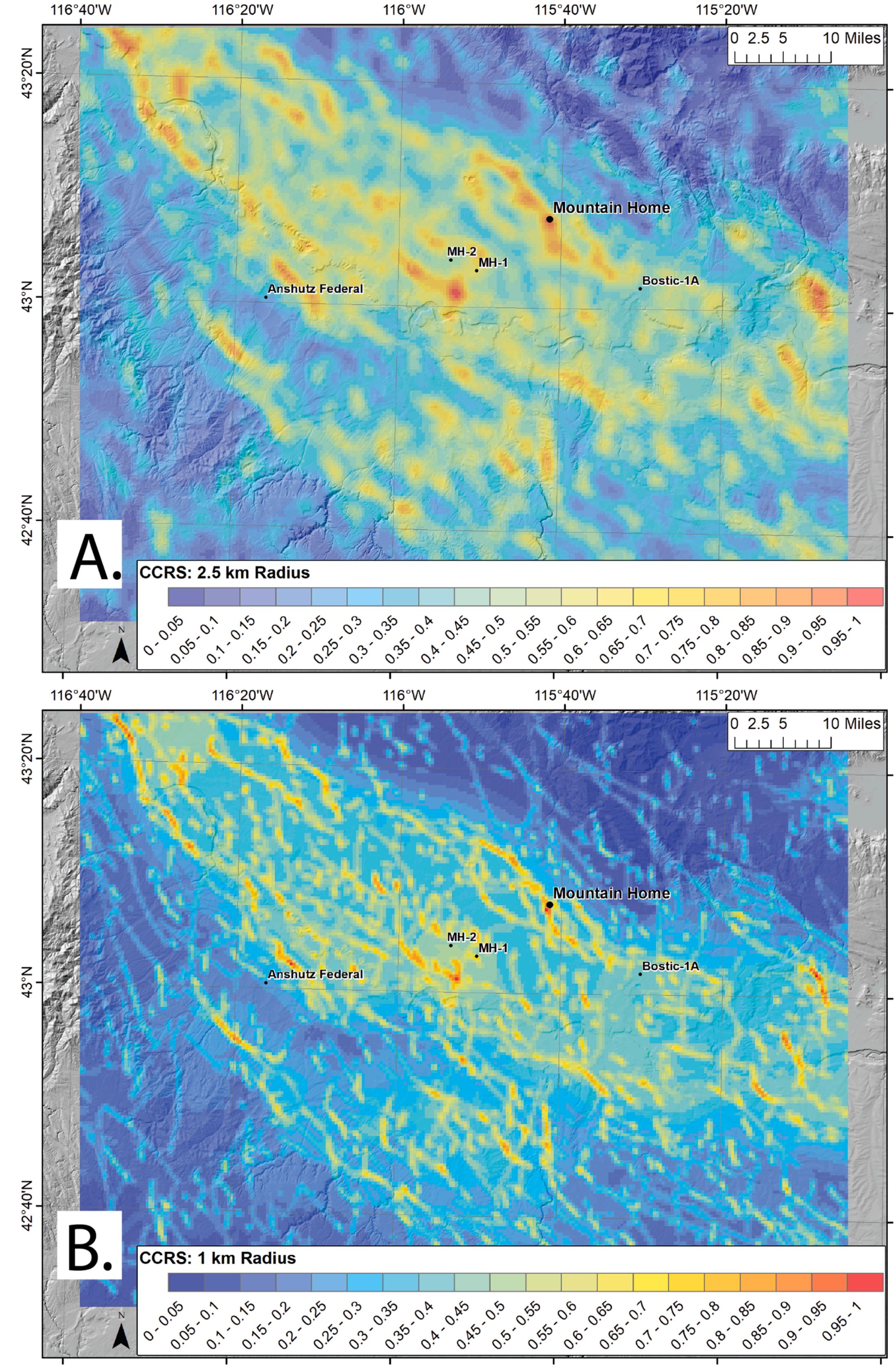

Fig. 7. Phase 2 CCRS maps for the WSRP illustrating the impact of using a higher resolution sampling grid (500 m) relative to Phase 1 (2 km), and changing the search radius of the kernel density function from 2.5 km (A) to 1 km (B). The larger search radius results in a more generalized map, whereas the smaller search radius begins to reflect individual lineaments in the permeability data. Hillshade from USGS 3D Elevation Program (U.S. Geological Survey, 2019).

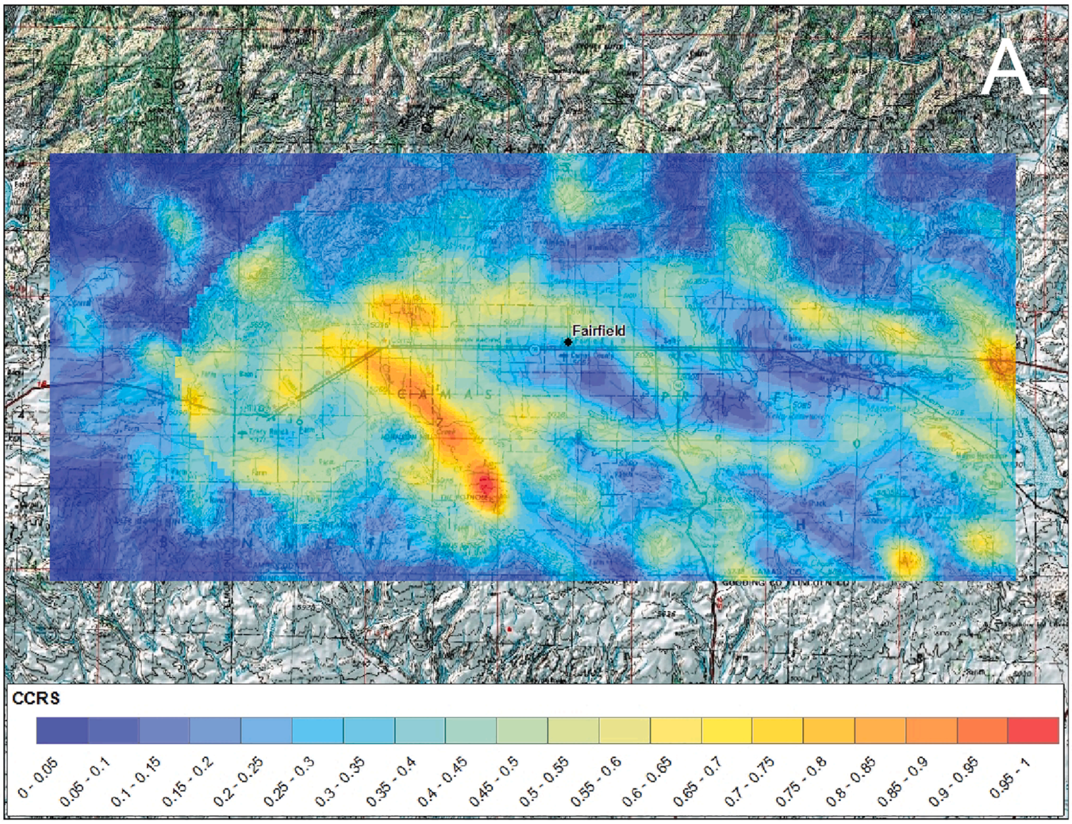

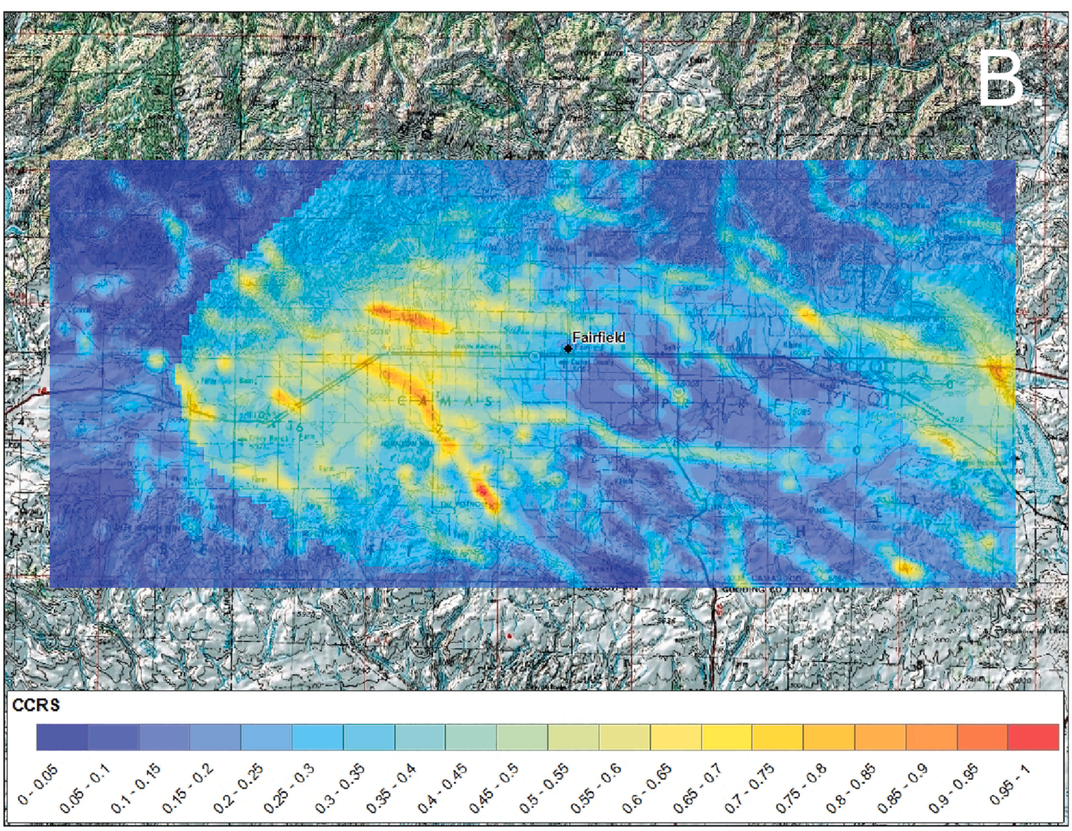

Fig. 8. Phase 2 CCRS maps for Camas Prairie constructed using Phase 2 wt and a 100 m sample grid. (A) CCRS map constructed using a search radius of 2.5 km in the kernel density function; (B) CCRS map constructed using a search radius of 1 km in the kernel density function. The smaller search radius highlights individual lineaments in the underlying permeability data. Hillshade from USGS 3D Elevation Program (U.S. Geological Survey, 2019).

geophysical data even allows its application to hidden or "blind" resources that are typically difficult to identity and target effectively. An important aspect of our approach is that it can easily be scaled from large regional studies (as presented here) to more localized areas, and that the evidence layers can be added or eliminated in response to the availability of data (DeAngelo et al., this volume). Furthermore, it is not restricted to exploration for traditional hydrothermal systems; it can be equally effective in locating suitable engineered geothermal prospects by combining the heat and seal CRS maps and using the permeability CRS map to eliminate areas with pre-existing permeability.

Our PFA of southern Idaho suggests that important undiscovered geothermal resources may be in several areas of the SRP. Our results identify eight areas with multiple prospects, each of which may contain resources that equal or exceed the 10 MW Raft River geothermal plant. Four of these areas are in the Western Snake River Plain (WSRP) and include blind systems; two are in the Central Snake River Plain (CSRP), and two are Basin and Range play types in eastern and southeastern Idaho. Our training site in the WSRP (on Mountain Home Air Force Base) has a confirmed resource that is at least 5 km long, parallel to a buried fault system. Our identified prospects exhibit higher favorability on *Common Risk Segment* and *Composite Common Risk Segment* maps than either of our training sites and have regional extents that generally exceed both of our training sites. These data strongly support the conclusion that commercial geothermal resources exceeding 100 MW are present in southern Idaho.

Idaho sits upon a unique geothermal resource that could potentially rival Nevada for power output. Our project has documented that prospective geothermal resources, fueled by volcanism in southern Idaho, are regional in distribution and may be tapped in zones of high permeability formed by faults. Many of these faults are exposed on the surface, but others are buried beneath thick blankets of clay-rich sediments that provide both a seal for the hot water resource and a layer of insulation for the underlying thermal anomaly. Older faults are also obscured by extensive, young volcanic flows that cover much of this region.

The goal of our project was to reduce the risk for private developers and thus remove barriers to further exploration and development. The methodology and tools developed by this project have helped to identify where these resources are most likely located, to estimate their volume, and in time, to locate the best places to drill in order to harness this resource. Furthermore, these methods and tools are transferable to other regions with different geothermal resources and may be used throughout the geothermal industry.

Submission declaration and verification

We certify that this work has not been published previously, that it is not under consideration for publication elsewhere, that its publication is approved by all authors and tacitly or explicitly by the responsible authorities where the work was carried out, and that, if accepted, it will not be published elsewhere in the same form, in English or in any other language, including electronically without the written consent of the copyright-holder.

CRediT authorship contribution statement

John W. Shervais: Project administration, Funding acquisition, Writing – original draft, Conceptualization, Methodology, Investigation, Resources, Formal analysis, Validation, Writing – review & editing. **Jacob DeAngelo:** Conceptualization, Methodology, Investigation, Resources, Formal analysis, Validation, Writing – review & editing. **Jonathan M. Glen:** Supervision, Funding acquisition, Conceptualization, Methodology, Investigation, Resources, Formal analysis, Validation, Writing – review & editing. **Dennis L. Nielson:** Conceptualization, Methodology, Investigation, Resources, Formal analysis, Validation, Writing – review & editing. **Sabodh Garg:** Conceptualization, Methodology, Investigation, Resources, Formal analysis, Validation, Writing – review & editing. **Patrick Dobson:** Supervision, Funding acquisition, Conceptualization, Methodology, Investigation, Resources, Formal analysis, Validation, Writing – review & editing. **Erika Gasperikova:** Conceptualization, Methodology, Investigation, Resources, Formal analysis, Validation, Writing – review & editing. **Eric Sonnenthal:** Conceptualization, Methodology, Investigation, Resources, Formal analysis, Validation, Writing – review & editing. **Lee M. Liberty:** Funding acquisition, Conceptualization, Methodology, Investigation, Resources, Formal analysis, Validation, Writing – review & editing. **Dennis L. Newell:** Conceptualization, Methodology, Investigation, Resources, Formal analysis, Validation, Writing – review & editing. **Drew Siler:** Conceptualization, Methodology, Investigation, Resources, Formal analysis, Validation, Writing – review & editing. **James P. Evans:** Conceptualization, Methodology, Investigation, Resources, Formal analysis, Validation, Writing – review & editing.

Declaration of Competing Interest

The authors declare that they have no known competing financial interests or personal relationships that could have appeared to influence the work reported in this paper.

Data availability

Data are available in the National Geothermal Data Repository; data links provided in the article.

Funding

This work was supported by U.S. Department of Energy Award EE-0006733. Further support was provided by Utah State University and the U.S. Geological Survey. This work was also supported with funding by the Assistant Secretary for Energy Efficiency and Renewable Energy, Geothermal Technologies Office, of the U.S. Department under the U.S. Department of Energy Contract No. DE-AC02-05CH11231 with Lawrence Berkeley National Laboratory.

Acknowledgments

We wish to thank Travis McLing and Ghanashyam Neupane (Idaho National Laboratory) and Tom Wood and Cody Cannon (University of Idaho) for generously sharing geothermometry results prior to publication, and our colleagues for stimulating discussions. Any use of trade, firm, or product names is for descriptive purposes only and does not imply endorsement by the U.S. Government.

Supplementary materials

Supplementary material associated with this article can be found, in the online version, at doi:10.1016/j.geothermics.2023.102865.

References

Anderson, SR, Akerman, DJ, Liszewski, MJ, 1996. USGS Open File Report OFR-96-248, p. 27.

Anderson, SR, Liszewski, MJ, Cecil, LD, 1997. USGS Water Resources Investigation Report 97-4010, p. 39.

Arney, B.H., 1982. Evidence of former higher temperatures from alteration minerals, Bostic 1-A well, Mountain Home, Idaho. Geother. Resourc. Council Transact. 6, 3–6.

Atkinson, T.A., Newell, D.L., Shervais, J.W., 2017. Petrographic and thermal evidence of high-temperature geothermal activity from the MH-2B slimhole, western Snake River Plain, Idaho. In: Proceedings, 42ndWorkshop on Geothermal Reservoir Engineering. Stanford University. February 2017.

Baker, S.J., Castelin, P.M., 1990. Idaho Department of Water Resources Water Information Bulletin, 30/16, p. 36.

Bankey, V., Cuevas, A., Daniels, D.L., Finn, C.A., Hernandez, I., Hill, P.L., Kucks, R., Miles, W., Pilkington, M., Roberts, C., Roest, W., 2002. Magnetic Anomaly Map of North America. US Geological Survey.

Barton, C.A., Zoback, M.D., Moos, D., 1995. Fluid flow along potentially active faults in crystalline rock. Geology 23, 23–27. https://doi.org/10.1130/0091-7613(1995)023<0683.

Barton, C.A., Hickman, S.H., Morin, R., Zoback, M.D., Benoit, D., 1998. Reservoir-scale fracture permeability in the Dixie Valley, Nevada, geothermal field. In: Proceedings, Soc. Pet. Eng. Annu. Meet., pp. 315–322. https://doi.org/10.2523/47371-MS.

Blackwell, D.D., Richards, M., 2004. Geothermal Map of North America. Amer. Assoc. Petroleum Geologists, Tulsa, Oklahoma, 1 sheet, scale 1:6,500,000.

Blackwell, D.D., Kelley, S.A., Steele, J.L., 1992. Heat Flow Modeling of the Snake River Plain, Idaho. Dept. of Geological Sciences, Southern Methodist University, US Department of Energy Contract DE-AC07-761DO1570, p. 109.

Blackwell, D.D., 1989. Regional implications of heat flow of the Snake River Plain, northwestern United States. Tectonophysics 164, 323–343 v.

Bonnichsen, B., 1982. The Bruneau-Jarbidge Eruptive Center, Southwestern Idaho, 26. Cenozoic Geology of Idaho: Idaho Bureau of Mines and Geology Bulletin, pp. 237–254.

Breckenridge, R.M., Lewis, R.S., Adema, G.W., Weisz, D.W., 2003. Miocene and Younger Faults in Idaho. Idaho Geological Survey Map. M-8; 1:1,000,000.

Breckenridge, RM, Gillerman, VS, Wray-Macomb, E., 2006. Oil and Gas Exploration in Idaho. Idaho Geological Survey. Digital Web Map 81.

Cannon, C., Wood, T., Neupane, G., McLing, T., Mattson, E., Dobson, P., Conrad, M., 2014. Geochemistry sampling for traditional and multicomponent equilibrium geothermometry in southeast Idaho. Geother. Resourc. Council Transact. 38, 425–431.

Conrad, M.E., Dobson, P.F., Sonnenthal, E.L., Kennedy, B.M., Cannon, C., Worthing, W., Wood, T., Neupane, G., Mattson, E., McLing, T., 2016. Application of isotopic approaches for identifying hidden systems in southern Idaho. In: Proceedings, 41st Workshop on Geothermal Reservoir Engineering, February 2016. Stanford, California. Stanford University.

Cumming, W., 2009. Geothermal resource conceptual models using surface exploration data. In: Proceedings, *34thWorkshop on* Geothermal Reservoir Engineering, February 2009. Stanford, California. Stanford University.

DeAngelo, J., Shervais, J.W., Glen, J.G., Dobson, P., Siler, D., Liberty, L.M., Gasperikova, E., Sonnenthal, E., Visser, C., Nielson, D.L., Garg, S., Evans, J.P., Santellanes, S., 2016, GIS Methodology for Play Fairway Analysis: example from the Snake River Plain Volcanic Province. Proceedings, *41st Workshop on Geothermal Reservoir Engineering, February 2016*, Stanford, California.

DeAngelo, J., Shervais, J.W., Glen, J.M., Dobson, P.F., Liberty, L.M., Siler, D.L., Neupane, G., Newell, D.L., Evans, J.P., Gasperikova, E., Peacock, J.R., Sonnenthal, E., Nielson, D.L., Garg, S.K., Schermerhorn, W.D., Earney, T.E., 2021a. Snake River Plain Play Fairway analysis phase 1 favorability model (DE EE0006733): US. Geological Surv. Data Releas. https://doi.org/10.5066/P95EULTI.

DeAngelo, J., Shervais, J.W., Glen, J.M., Dobson, P.F., Liberty, L.M., Siler, D.L., Neupane, G., Newell, D.L., Evans, J.P., Gasperikova, E., Peacock, J.R., Sonnenthal, E., Nielson, D.L., Garg, S.K., Schermerhorn, W.D., Earney, T.E., 2021b. Snake River Plain Play Fairway Analysis Phase 2 Favorability Model (DE EE0006733). US. Geological Survey data release. https://doi.org/10.5066/P9Y8MEZY.

DeNosaquo, K.R., Smith, R.B., Lowry, A.R., 2009. Density and lithospheric strength models of the Yellowstone-Snake River Plain volcanic system from gravity and heat flow data. J. Volcanol. Geotherm. Res. 188, 108–127, 2009.

Desborough, GA, Raymond, W.H., Marvin, R.F., Kellogg, K.S., 1989. Open-File Report 89-436, p. 18.

Dezayes, C., Famin, V., Tourlière, B., Baltassat, J.M., Bénard, B., 2022. Potential areas of interest for the development of geothermal energy in La Réunion Island based on GIS analysis. J. Volcanol. Geotherm. Res. 421, 107450.

Dobson, P.F., Kennedy, B.M., Conrad, M.E., McLing, T., Mattson, E., Wood, T., Cannon, C., Spackman, R., van Soest, M., Robertson, M., 2015. He isotopic evidence for undiscovered geothermal systems in the Snake River Plain. In: Proceedings, 40th Workshop on Geothermal Reservoir Engineering. Stanford, CA. Stanford University, p. 7.

Doherty, D.J., McBroome, L.A., Kuntz, M.A., 1979. Preliminary geological interpretation and lithologic log of the exploratory geothermal test well (INEL-1), Idaho National Engineering Laboratory, eastern Snake River Plain, Idaho. USGS Open File Report OFR-79-1248, p. 9.

Doherty, D.J., 1979. Drilling data from exploration well 1, NE 1/4, sec. 22, T. 2 N., R. 32 E., Bingham County, Idaho. USGS Open File Report OFR-79-1225, plate.

Embree, G.F., Lovell, M.D., Doherty, D.J., 1978. Drilling data from Sugar City exploration well, Madison County, Idaho. USGS Open File Report OFR78-1095, plate.

Facca, G., Tonani, F., 1967. The self-sealing geothermal field. Bull. Volcanol. 30, 271–273.

Faulds, J.E., Hinz, N.H., Dering, G.M., Siler, D.L., 2013. The hybrid model-the most accommodating structural setting for geothermal power generation in the Great Basin, Western USA. Geotherm. Resourc. Counc. Transact. 37, 3–10.

Ferrill, D.A., Winterle, J., Wittmeyer, G., Sims, D., Colton, S., Armstrong, A., Horowitz, A. S., Meyers, W.B., Simons, F.F., 1999. Stressed rock strains groundwater at Yucca Mountain, Nevada. GSA Today 9, 2–9.

Fleischmann, D.J., 2006. Geothermal Development Needs in Idaho. Geothermal Energy Association, p. 51.

Fugelli, E.M.G., Olsen, T.R., 2005. Risk assessment and play fairway analysis in frontier basins: part 2 – examples from offshore mid-Norway. Am. Assoc. Pet. Geol. Bull. 89 (7), 883–896.

Gao, H., Humphreys, E.D., Yao, H., van der Hilst, R.D., 2011. Crust and lithosphere structure of the Northwestern U.S. with ambient noise tomography: terrane accretion and Cascade arc development. Earth Planet. Sci. Lett. https://doi.org/10.1016/j.epsl.2011.01.033.

Garabedian, S.P., 1992. Hydrology and digital simulation of the regional aquifer system, eastern Snake River Plain, Idaho. USGS Professional Paper 1408F. p. 102 10 Plates.

Garg, S.K., Nielson, D.L., Shervais, J.W., Sonnenthal, E., 2016. Thermal modeling of the Mountain Home Geothermal Area. In: Proceedings, *41st Workshop on Geothermal Reservoir Engineering, February 22-24, 2016*. Stanford, California. Stanford University. SGP-TR-209.

Getman, D., Anderson, A., Augustine, C., 2015. Geothermal Prospector: supporting geothermal analysis through spatial data visualization and querying tools. Geotherm. Resourc. Council Transact. 39, 977–986 v.

Glen, JMG, Liberty, L, Gasperikova, E, Siler, D, Shervais, JW, Ritzinger, B, Athens, N, Earney, T, 2017. Geophysical Investigations and Structural Framework of Geothermal Systems in west and southcentral Idaho; Camas Prairie to Mountain Home. In: Proceedings, 42nd Workshop on Geothermal Reservoir Engineering, February 13-15, 2017. Stanford University, Stanford, California. SGP-TR-212.

Grant, M.A., Bixley, P.F., 2011. Geothermal Reservoir Engineering, 2nd Edition. Academic Press, Burlington MA. ISBN: 978-0-12-383880-3.

Grant, S., N. Milton, and M. Thompson, 1996, Play fairway analysis and risk mapping: an example using the Middle Jurassic Brent Group in the northern North Sea, in A. G. Dore and R. Sinding- Larsen, eds., Quantification and Prediction of Petroleum Resources: Norwegian Petroleum Society Special Publication 6, p. 167–181.

Hackett, W.R., Anders, M., Walter, R.C., 1994. Preliminary stratigraphic framework of rhyolites from corehole WO-2, Idaho National Engineering Laboratory: caldera-related late Tertiary Silicic volcanism in the eastern Snake River plain, Abstracts. In: VIIth International Symposium on the Observation of Continental Crust Through Drilling. Santa Fe, New Mexico, 1994.

Helm-Clark, C.M., Rodgers, D.W., Smith, RP, 2004. Borehole geophysical techniques to define stratigraphy, alteration and aquifers in basalt. J. Appl. Geophy. 55, 3–38 v.

Hill DP and Pakiser, LC, 1967 Crustal structure between the Nevada test site and Boise Idaho from seismic refraction measurements, in Steinhart and Smith (eds), The Earth beneath the Continents: American Geophysical Union Monograph 10, (1967), 391–419.

Ito, T., Zoback, M.D., 2000. Fracture permeability and *in situ* stress to 7 km depth in the KTB scientific drillhole. Geophys. Res. Lett. 27 (7), 1045–1048.

Ito, G., Frazer, N., Lautze, N., Thomas, D., Hinz, N., Waller, D., Whittier, R., Wallin, E., 2017. Play fairway analysis of geothermal resources across the state of Hawaii: 2. Resource probability mapping. Geothermics 70, 393–405. https://doi.org/10.1016/j.geothermics.2016.11.004.

Iwahashi, G.S., Hughes, S.S., 2006. Anomalous geologic setting of the spencer-high point volcanic field, Eastern Snake River Plain, Idaho. In: AGU Fall Meeting Abstracts, 2006, pp. V51D–1708.

Iwahashi, G.S., 2010. Physical and compositional implications for the evolution of Spencer-High Point Volcanic Field. MSc thesis. Idaho State University, Idaho, p. 179.

Jean, MM, Shervais, JW, Champion, DE, Vetter, SK, 2013. Geochemical and paleomagnetic variations in basalts from the Wendell Regional Aquifer Systems Analysis (RASA) drill core: evidence for magma recharge and assimilation–fractionation crystallization from the central Snake River Plain, Idaho. Geosphere. https://doi.org/10.1130/GES00914.1.

Kelbert, A., Egbert, G.D., deGroot-Hedlin, C., 2012. Crust and upper mantle electrical conductivity beneath the Yellowstone Hotspot Track. Geology 40 (5), 447–450.

Kessler, JA, Bradbury, KK, Schmitt, DR, Shervais, JW, Pulsipher, MA, Rowe, FE, Varriale, JA, Evans, JP, 2017. Geology and *in situ* stress of the MH-2 Borehole, Idaho, U.S.A.: insights into Western Snake River Plain Structure from Geothermal Exploration Drilling. Lithosphere. https://doi.org/10.1130/L609.1.

Kuntz, MA, Champion, DE, Spiker, EC, Lefebvre, RH, 1986a. Contrasting magma types and steady-state, volume predictable, basaltic volcanism along the Great Rift, Idaho. Geol. Soc. Am. Bull. 87, 579–594.

Kuntz, M.A., Spiker, E.C., Rubin, M., Champion, D.E., Lefebvre, R.H., 1986b. Radiocarbon studies of latest Pleistocene and Holocene lava flows of the Snake River Plain, Idaho: data, lessons, interpretations. Quat. Res. 25 (2), 163–176.

Kuntz, M.A., Anderson, S.R., Champion, D.E., Lanphere, M.A., Grunwald, D.J. 2002, Pleistocene-Holocene basaltic volcanism and implications for the distribution of hydraulic conductivity in the eastern Snake River Plain, Idaho, Link, P.K., Mink, L.L. *Geology, Hydrogeology, and Environmental Remediation: Idaho National Engineering and Environmental Laboratory, Eastern Snake River Plain, Idaho:* Geological Society of America Special Paper 353, 2002, 111–133.

Lachmar, T.E., Freeman, T.G., Sant, C.J., Walker, J.R., Batir, J.F., Shervais, J.W., Evans, J.P., Nielson, D.L., Blackwell, D.D., 2017. Effect of an 860-m thick, cold, freshwater aquifer on geothermal potential along the axis of the eastern Snake River Plain, Idaho. Geothermal Energy 5, 28.

Lachmar, T.E., Freeman, T.G., Kessler, J.A., Batir, J.F., Evans, J.P., Nielson, D.L., Shervais, J.W., Chen, X., Schmitt, D.R., Blackwell, D.D., 2019. Evaluation of the geothermal potential of the western Snake River Plain based on a deep corehole on the Mountain Home AFB near Mountain Home, Idaho. Geothermal Energy 7, 26.

Lautze, N., Thomas, D., Hinz, N., Apuzen-Ito, G., Frazer, N., Waller, D., 2017a. Play fairway analysis of geothermal resources across the State of Hawaii: 1. Geological, geophysical, and geochemical datasets. Geothermics 70, 376–392. https://doi.org/10.1016/j.geothermics.2017.02.001.

Lautze, N., Thomas, D., Waller, D., Frazer, N., Hinz, N., Apuzen-Ito, G., 2017b. Play fairway analysis of geothermal resources across the state of Hawaii: 3. Use of development viability criterion to prioritize future exploration targets. Geothermics 70, 406–413. https://doi.org/10.1016/j.geothermics.2017.07.005.

Lewis, R.E., Stone, M.A.J., 1988. Geohydrologic data from a 4,403-foot geothermal test hole, Mountain Home Air Force Base, Elmore County. Open File Report, 34. US Geological Survey, Idaho, pp. 88–166.

Lewis, R.E., Young, H.W., 1989. The hydrothermal system in central Twin Falls County, Idaho. U.S. Geological Survey Water-Resources Investigations Report 88-4152, p. 44.

Lindholm, G.F., 1996. Summary of the Snake River regional aquifer-system analysis in Idaho and eastern Oregon: U.S. Geological Survey Professional Paper 1408-A, p. 59.

Machette, M.N., Haller, K.M., Dart, R.L., Rhea, S.B., 2003. U.S. Geological Survey Open-File Report 03-417. https://doi.org/10.3133/ofr03417.

Manley, C.R., 1996. Physical volcanology of a voluminous rhyolite lava flow: the Badlands lava, Owyhee Plateau, southwestern Idaho. J. Volcanol. Geotherm. Res. 71 (2-4), 129–153.

McCafferty, A.E., Kucks, R.P., Hill, P.L., Racey, S.D., 1999. US Geological Survey Open-File Report 99-371. https://doi.org/10.3133/ofr99371.

McCurry, M., Welhan, J., 2012. Do Magmatic-related geothermal energy resources exist in southeast Idaho. Geotherm. Resourc. Council Transact. 36, 699–707 v.

McCurry, M., Hayden, K.P., Morse, L.H., Mertzman, S., 2008. Genesis of post-hotspot, A-type rhyolite of the Eastern Snake River Plain volcanic field by extreme fractional crystallization of olivine tholeiite. Bull. Volcanol. 70, 361–383.

McCurry, M, Welhan, J, Polun, S, Autenrieth-Rodgers, DW, 2011. Geothermal potential of the Blackfoot Reservoir-Soda Springs volcanic field: hidden geothermal resource and natural laboratory in SE Idaho. Geothermal Resources Council Transactions 35, 917–924.

McCurry, M., Pearson, DM, Welhan, J, Natwotniak, SK, Fisher, M., 2015. Origin and potential geothermal significance of China Hat and other late Pleistocene Topaz Rhyolite Lava domes of the Blackfoot Volcanic Field, SE Idaho. Geotherm. Resourc. Council Transact. 39, 2–5.

McIntyre, D.H., 1979. Preliminary description of Anschutz Federal No. 1 Drill Hole, Owyhee County, Idaho. USGS Open File Report OFR 79-651, p. 15.

McLing, TL, Smith, RW, Johnson, TM, 2002. Chemical Characteristics of Thermal Water beneath the Eastern Snake River Plain. In: Link, PK., Mink, LL (Eds.), Geology, Hydrogeology, and Environmental Remediation: Idaho National Engineering and Environmental Laboratory, Eastern Snake River Plain, Idaho. Geological Society of America, pp. 205–211. Special Paper 353.

McLing, T., McCurry, M., Cannon, C., Neupane, G., Wood, T., Podgorney, R., Welhan, J., Mines, G., Mattson, E., Palmer, G., Smith, R., 2014. David Blackwell's forty years in the Idaho Desert, the foundation for 21st Century geothermal research. Geothermal Resources Council Transactions 38, 143–153.

McLing, T.L., Smith, R.P., Smith, R.W., Blackwell, D.D., Roback, R.C., Sondrup, A.J., 2016. Wellbore and groundwater temperature distribution eastern Snake River Plain, Idaho: implications for groundwater flow and geothermal potential. J. Volcanol. Geotherm. Res. 320, 144–155.

Moeck, I.S., 2014. Catalog of geothermal play types based on geologic controls. Renew. Sustain. Energy Rev. 37, 867–882.

Morris, A., Ferrill, D.A., Henderson, D.B., 1996. Slip-tendency analysis and fault reactivation. Geology 24, 275–278.

Morse, L.H., and McCurry, M., 2002, Genesis of alteration of quaternary basalts within a portion of the eastern Snake River Plain Aquifer. In Link, P.K., and Mink, L.L., (Eds.), *Geology, Hydrogeology, and Environmental Remediation; Idaho National Engineering and Environmental Laboratory, Eastern Snake River Plain, Idaho*. GSA Special Paper, 353: 213–224.

Neber, A., Cox, S., Levy, T., Schenk, O., Tessen, N., Wygrala, B., Bryant, I., 2012. Systematic evaluation of unconventional resource plays using a new play-based exploration methodology. In: SPE Asia Pacific Oil and Gas Conference and Exhibition, October. Perth, Australia. https://doi.org/10.2118/158571-MS.

Neely, K.W., 1996. Geothermal heat keeps students warm at the College of Southern Idaho. Geotherm. Resourc. Council Transact. 20, 129–136.

Neupane, G., Mattson, E.D., McLing, T.L., Palmer, C.D., Smith, R.W., Wood, T.R., 2014. Deep geothermal reservoir temperatures in the Eastern Snake River Plain, Idaho using multicomponent geothermometry. In: Proceedings, *38th Workshop on Geothermal Reservoir Engineering, February 24-26, 2014*. Stanford, California. Stanford University. SGP-TR-202.

Neupane, G., Mattson, E.D., Spycher, N., Dobson, P.F., Conrad, M.E., Newell, D.L., McLing, T.L., Wood, T.R., Cannon, C.J., Atkinson, T.A., Brazell, C.W., 2017. Geochemical evaluation of the geothermal resources of Camas Prairie, Idaho. In: Proceedings, *42nd workshop on geothermal reservoir engineering*. Stanford, California. Stanford University.

Newton, G.D., 1991. Geohydrology of the Regional Aquifer system, Western Snake River Plain, Southwestern Idaho, 1408. US Government Printing Office.

Nielson, DL, Shervais, JW, 2014. Conceptual model for Snake River Plain geothermal systems. In: Proceedings, *39th Workshop Geothermal Reservoir Engineering*. Stanford University. SGP-TR-202.

Nielson, DL, Delahunty, C, Shervais, JW, 2012. Geothermal systems in the Snake River Plain, Idaho, characterized by the Hotspot project. Geothermal Resources Council Transactions 36, 727–730.

Nielson, D.L., Shervais, J.W., Evans, J.P., Liberty, L., Garg, S.K., Glen, J., Visser, C., Dobson, P., Gasperikova, E., Sonnenthal, E., 2015. Geothermal Play Fairway Analysis of The Snake River Plain, Idaho. Stanford University, Stanford, California. January 26-28, 2015 SGP-TR-204.

Nielson, D.L., Sonnenthal, E., Shervais, J.W., Garg, S.K., 2017. Mafic heat sources for Snake River Plain geothermal systems. In: Proceedings of the 42nd workshop on geothermal reservoir engineering. Stanford, pp. 1205–1212.

Noorollahi, Y., Itoi, R., Fujii, H., Tanaka, T., 2008. GIS integration model for geothermal exploration and well siting. Geothermics 37 (2), 107–131.

Palmer, C.D., Ohly, S.R, Smith, R.W., Neupane, G., McLing, T., Mattson, E., 2014. Mineral selection for multicomponent equilibrium geothermometry. Geotherm. Resourc. Council Transact. 38, 453–459..

Payne, SJ, McCaffrey, R, King, RW, 2008. Strain rates and contemporary deformation in the Snake River Plain and surrounding Basin and Range from GPS and seismicity. Geol. Soc. Am. Bull. 36 (8), 647–650.

Payne, S.J., McCaffrey, R., King, R.W., Kattenhorn, S.A., 2012. A new interpretation of deformation rates in the Snake River Plain and adjacent basin and range regions based on GPS measurements. Geophys. J. Int. 189 (1), 101–122. https://doi.org/10.1111/j.1365-246X.2012.05370.x pages.

Payne, S.J., McCaffrey, R., Kattenhorn, S.A., 2013. Extension-driven right-lateral shear in the Centennial shear zone adjacent to the eastern Snake River Plain. Idaho. Lithosphere 5 (4), 407–419.

Peng, X., Humphreys, E.D., 1998. Crustal velocity structure across the eastern Snake River plain and the Yellowstone Swell. J. Geophys. Res. 7171–7186, 103/4, 1998).

Phillips, WM, Welhan, JA, 2006. Geologic Map of the Idaho Falls North Quadrangle, Bonneville County, Idaho. Idaho Geological Survey. Digital Web Map DWM-77, 1: 24,000.

Phillips, WM, Welhan, JA, 2011. Geologic Map of the Idaho Falls South Quadrangle, Bingham and Bonneville County, Idaho. Idaho Geological Survey. Digital Web Map DWM-78, 1:24,000.

Potter, KA, Shervais, JW, Christiansen, EH, Vetter, SK, 2018. Evidence for cyclical fractional crystallization, recharge, and assimilation in basalts of the Kimama drill core, central Snake River Plain, Idaho: 5.5-million-years of petrogenesis in a mid-crustal sill complex. Front. Earth Sci. https://doi.org/10.3389/feart.2018.00010.

Potter, K.E., Champion, D.E., Duncan, R.A., Shervais, J.W., 2019. Volcanic stratigraphy and age model of the Kimama deep borehole (Project Hotspot): evidence for 5.8 million years of continuous basalt volcanism, central Snake River Plain, Idaho. Geosphere 15, 1–23. https://doi.org/10.1130/GES01679.1.

Prol-Ledesma, R.M., 2000. Evaluation of the reconnaissance results in geothermal exploration using GIS. Geothermics 29 (1), 83–103.

Sant, C.J., 2012. Geothermal Alteration of Basaltic Core from the Snake River Plain, Idaho. M.Sc. Thesis. Utah State University, p. 113.

Shell Exploration & Production, 2013. Play Based Exploration Guide. Graphics Media and Publishing Services (GMP), Rijswijk, Netherlands.

Shervais, J.W., Kauffman, J.D., Gillerman, V.S., Othberg, K.L., Vetter, S.K., Hobson, V.R., Meghan Zarnetske, M., Cooke, M.F., Matthews, S.H., and Hanan, B.B., 2005, Basaltic volcanism of the Central and Western Snake River Plain: a guide to field relations between Twin Falls and Mountain Home, Idaho; in J. Pederson and C.M. Dehler, *Guide to Field trips in the Western United States, Field Guide volume* 6, Geological Society of America, Boulder Colorado, 26.

Shervais, J.W., Vetter, S.K., Hanan, B.B., 2006. A layered mafic sill complex beneath the Eastern Snake River Plain: evidence from cyclic geochemical variations in basalt. Geology 34, 365–368. https://doi.org/10.1130/G22226.1.

Shervais, J.W., Schmitt, D.R., Nielson, D.L., Evans, J.P., Christiansen, E.H., Morgan, L., Shanks, W.C.P., Lachmar, T., Liberty, L.M., Blackwell, D.D., Glen, J.M., Champion, D., Potter, K.E., Kessler, J.A., 2013. First results from HOTSPOT: The Snake River Plain Scientific Drilling Project, Idaho, USA. Sci. Drill. 15 https://doi.org/10.2204/iodp.sd.15.06.2013.

Shervais, J.W., Evans, J.P., Schmitt, D., Christiansen, E.H., Prokopenko, A., 2014. HOTSPOT: The Snake River Scientific Drilling Project. EOS, Transactions American Geophysical Union 95, 85–86. https://doi.org/10.1002/2014EO100001.

Shervais, JW, Glen, JM, Nielson, DL, Garg, S, Liberty, LM, Siler, D, Dobson, PF, Gasperikova, E, Sonnenthal, E, Neupane, G, DeAngelo, J, Newell, DL, Evans, JP, Snyder, N, 2017. Geothermal play fairway analysis of the Snake River Plain: phase 2. Geothermal Resources Council Transactions 41, 2352–2369.

Shervais, JW, Glen, JM, Siler, D, Deangelo, J, Liberty, LM, Nielson, DL, Garg, S, Neupane, G., Dobson, P, Gasperikova, E, Sonnenthal, E, Newell, DL, Evans, JP, Snyder, N, Mink, LL, 2018. Provisional conceptual model of the camas prairie (ID) geothermal system from play fairway analysis. In: Proceedings, 43rd Workshop on Geothermal Reservoir Engineering, February 12-14, 2018. Stanford, California. Stanford University. SGP-TR-213.

Sibson, R.H., 1994. Crustal stress, faulting and fluid flow. In: Parnell, J. (Ed.), Geofluids: Origin, Migration and Evolution of Fluids in Sedimentary Basins. Geological Society, London, pp. 69–84. *Special Publications*.

Sibson, H., 1996. Structural permeability of fluid-driven fault-fracture. J. Struct. Geol. 18, 1031–1042.

Siler, D.L., Faulds, J.E., Mayhew, B., McNamara, D.D., 2016. Analysis of the favorability for geothermal fluid flow in 3D: astor Pass geothermal prospect, Great Basin, northwestern Nevada, USA. Geothermics 60, 1–12.

Smith, R.B., Jordan, M., Steinberger, B., Puskas, C.M., Farrell, J., Waite, G.P., Husen, S., Chang, W.L., O'Connell, R., 2009. Geodynamics of the Yellowstone hotspot and mantle plume: seismic and GPS imaging, kinematics, and mantle flow. J. Volcanol. Geotherm. Res. 188 (1-3), 26–56.

Smith, RP, 2004. Geologic setting of the Snake River Plain Aquifer and vadose zone. Vadose Zone J. 3, 47–58.

Sparlin, MA, Braile, LW, Smith, RB, 1982. Crustal structure of the eastern Snake River Plain determined from ray trace modeling of seismic refraction data. J. Geophys. Res. 87, 2619–2633.

Spycher, N., Peiffer, L., Sonnenthal, E., Saldi, G., Reed, M.H., Kennedy, B.M., 2014. Integrated multicomponent solute geothermometry. Geothermics 51, 113–123.

Stanley, W.D., Boehl, J.E., Bostick, F.X., Smith, H.W., 1977. Geothermal significance of magnetotelluric sounding in the Eastern Snake River Plain-Yellowstone region. J. Geophys. Res. 82, 2501–2514, 1977.

Starks, S.A., Keller, G.R., Cooke, D.E., 1997. Pan-American Center for Earth and Environmental Studies. Earth and Environmental Remote Sensing at PACES, Vol. 12. Geocarto international.

Street, L.V., DeTar, R.E., 1987. Geothermal Resource Analysis in Twin Falls County, Idaho, in Geothermal Investigations in Idaho, IDWR Water Information Bulletin No. 30, Part 15. Geothermal Investigations in Idaho, p. 46.

Street, L.V., 1990. Geothermal resource analysis in the Big Wood River Valley, Blaine County, Idaho. IDWR Water Information Bulletin No. 30, Part 17, p. 26, 1 plate.

Taubeneck, W.H., 1971. Idaho batholith and its southern extension. Geol. Soc. Am. Bull. 82 (7), 1899–1928.

Townend, J., Zoback, M.D., 2000. How faulting keeps the crust strong. Geology 28, 399–402. https://doi.org/10.1130/0091-7613(2000)28<399:HFKTCS>2.0.CO.

Trumpy, E., Donato, A., Gianelli, G., Gola, G., Minissale, A., Montanari, D., Santilano, A., Manzella, A., 2015. Data integration and favourability maps for exploring geothermal systems in Sicily, southern Italy. Geothermics 56, 1–16.

Walker, J.D., Sabin, A.E., Unruh, J.R., Combs, J., Monastero, F.C., 2005. Development of genetic occurrence models for geothermal prospecting. Geotherm. Resourc. Council Transact. 29, 309–313.

Ward, SH, Ross, HP, Nielson, DL, 1981. Exploration strategy for high temperature hydrothermal systems in the Basin and Range Province. Am. Assoc. Petrol. Geolog. Bull. 65/1, 86102.

Welhan, J.A., Clemo, T.M., Gego, E.L., 2002. Stochastic simulation of aquifer heterogeneity in a layered basalt aquifer system, Snake River Plain, Idaho. In: Link, PK., Mink, LL (Eds.), Geology, Hydrogeology, and Environmental Remediation: Idaho National Engineering and Environmental Laboratory, Eastern Snake River Plain, Idaho. Geological Society of America, pp. 225–248. Special Paper 353.

Welhan, J.A., Gwyunn, M., Payne, S., McCurry, M., Plummer, M., Wood, T., 2014. The Blackfoot volcanic field, southeast Idaho: a hidden high-temperature geothermal resource in the Idaho thrust belt. In: Proceedings of the 39th Workshop on Geothermal Reservoir Engineering Stanford University, February. Stanford, California, 2426.

Welhan, J.A., 2016. Gigawatt-scale power potential of a magma-supported geothermal system in the fold and thrust belt of southeast Idaho. In: Proceedings, 41st Workshop on Geothermal Reservoir Engineering, February 2016. Stanford, California, p. 13. SGP-TR-209.

Wetmore, P.H., Hughes, S.S., Connor, L.J., Caplinger, M.L., Connor, C., 2009. Spatial distribution of eruptive centers about the Idaho National Laboratory. Volcanic and Tectonic Hazard Assessment for Nuclear Facilities, 229256.

Whitehead, R.L., Lindholm, G.F., 1985. Results of Geohydrologic Test Drilling in the Eastern Snake River Plain, Gooding County, Idaho. US Geological Survey Water-Resources Investigations Report 84-4294.

Whitehead, R.L., 1986. Geohydrologic framework of the Snake River basin, Idaho and eastern Oregon. U.S. Geological Survey Hydrologic Investigations Atlas. HA-681scale 1:1,000,000, 3 sheets.

Whitehead, R.L., 1992. Geohydrologic framework of the Snake River Plain regional aquifer system, Idaho and eastern Oregon (No. 1408-B). US Government Printing Office.

Williams, C.F., DeAngelo, J., 2008. Mapping geothermal potential in the Western United States. Geotherm. Resourc. Counc. Transact. 32, 181–188.

Williams, C.F., DeAngelo, J., 2011. Evaluation of approaches and associated uncertainties in the estimation of temperatures in the upper crust of the western United States. Geotherm. Resourc. Council Transact. 35, 1599–1605.

Wood, S.H., Anderson, J.E., 1981. Part II: Geological, Hydrological, and Geochemical and Geophysical Investigation of the Nampa-Caldwell and the Adjacent areas, Southwestern Idaho. Geothermal Investigations in Idaho, Idaho Department of Water Resources.

Wood, S.H., Clemens, D.M., 2002. Geologic and tectonic history of the western Snake River Plain, Idaho and Oregon. In: Bonnichsen, B., White, C., McCurry, M. (Eds.), Tectonic and Magmatic Evolution of the Snake River Plain volcanic Province. Idaho Geological Survey Bulletin 30, Moscow, ID, United States, pp. 69–103.

Wood, S.H., 1994. Seismic expression and geological significance of a lacustrine delta in Neogene deposits of the western Snake River plain, Idaho. Am. Assoc. Pet. Geol. Bull. 78 (1), 102–121.

Young, H.W., Mitchell, J.C., 1973. Idaho Department of Water Administration Water Information Bulletin No. 30, p. 43.

Zoback, M.D., Townend, J., 2001. Implications of hydrostatic pore pressures and high crustal strength for the deformation of intraplate lithosphere. Tectonophysics 336, 19–30. https://doi.org/10.1016/S0040-1951(01)00091-9.